



THE UNIVERSITY *of* EDINBURGH

Edinburgh Research Explorer

Integrated analysis of Wnt signalling system component gene expression

Citation for published version:

Murphy, P, Armit, C, Hill, B, Venkataraman, S, Frankel, P, Baldock, R & Davidson, D 2022, 'Integrated analysis of Wnt signalling system component gene expression', *Development*.
<https://doi.org/10.1242/dev.200312>

Digital Object Identifier (DOI):

[10.1242/dev.200312](https://doi.org/10.1242/dev.200312)

Link:

[Link to publication record in Edinburgh Research Explorer](#)

Document Version:

Peer reviewed version

Published In:

Development

General rights

Copyright for the publications made accessible via the Edinburgh Research Explorer is retained by the author(s) and / or other copyright owners and it is a condition of accessing these publications that users recognise and abide by the legal requirements associated with these rights.

Take down policy

The University of Edinburgh has made every reasonable effort to ensure that Edinburgh Research Explorer content complies with UK legislation. If you believe that the public display of this file breaches copyright please contact openaccess@ed.ac.uk providing details, and we will remove access to the work immediately and investigate your claim.



Integrated analysis of Wnt signalling system component gene expression

Paula Murphy^{1,*}, Chris Armit^{2,3}, Bill Hill², S. Venkataraman², Patrick Frankel¹, Richard Baldock² and Duncan Davidson²

¹School of Natural Sciences, Trinity College Dublin, The University of Dublin, Dublin 2, Ireland

²MRC Human Genetics Unit, Institute of Cancer and Genetics, University of Edinburgh, Crewe Road EH4 2XU Edinburgh, UK

*Address for correspondence: Paula Murphy, Zoology, Trinity College Dublin, Ireland.
Phone: +353-1-896-3780; Fax: +353-677-8094; E-mail: paula.murphy@tcd.ie

‡Present address; BGI Hong Kong, 26/F, Kings Wing Plaza 2, 1 On Kwan Street, Shek Mun, NT, Hong Kong

Key words: Wnt signaling; 3D imaging; integrated analysis; computational analysis

ABSTRACT

Wnt signalling controls patterning and differentiation across many tissues and organs of the developing embryo via temporally and spatially restricted expression of multi-gene families encoding ligands, receptors, pathway modulators and intracellular components. Here we report an integrated analysis of key encoding genes in the 3D space of the mouse embryo across multiple stages of development. We applied a method for 3D/3D image transformation to map all gene expression patterns to a single reference embryo for each stage providing both visual analysis and volumetric mapping allowing computational methods to interrogate the combined expression patterns. We identify novel territories where multiple Wnt and Fzd genes are co-expressed and cross-compare all patterns, including all seven Wnt paralogous gene pairs. The comprehensive analysis allows regions

in the embryo where no Wnt or Fzd gene expression is detected, and where single Wnt genes are uniquely expressed, to be revealed. This work provides insight into a level of organisation of the patterns not previously possible, as well as presenting a resource that can be utilised further by the research community for whole system analysis.

INTRODUCTION

The Wnt signalling system of cell-cell communication is ancient and fundamental to the construction of an organised animal body plan (Loh et al., 2016), proposed to have arisen concurrently with the metazoan lineage (Moroz et al., 2014; Ryan et al., 2013). Since the original dual discoveries of key roles for Wnt in development and dysregulation during oncogenic transformation, it has more recently been shown to control cell differentiation within, and maintenance of, stem cell niches (Clevers et al., 2014). Spatio-temporally localised Wnt signalling plays a key role in patterning the primary body axis across very different body plans (Holstein, 2012) and is required for the establishment and healthy maintenance of organ systems from the Central Nervous System (CNS) to the kidney and gut (Noelanders and Vleminckx, 2017; Tian et al., 2018; Wang et al., 2018). Clearly, the spatio-temporal expression of genes that control Wnt signalling is of central importance.

The Wnt system is complex, with components encoded by several highly conserved multi-gene families; for example, there are 19 conserved Wnt ligand encoding genes in all mammals. Indeed, Wnts are unusual with respect to the high number of family members and paired paralogues, compared for example to the hedgehog family, with only three vertebrate members. FGFs are another example of a large family of signaling-molecule-encoding-genes present early in multicellular evolution, like Wnts; however, their classification into direct paralogous pairs is less clear (Itoh and Ornitz, 2011). Each Wnt is uniquely essential as demonstrated by mutation analysis in the mouse and the level of sequence conservation between species. 10 genes encode Frizzled (Fzd) receptors, that work together with a variety of co-receptors such as Lrps, Ryk and Ror. Extra-cellular modulators of the pathways include Secreted Frizzled Related Proteins (Sfrps), Wif and Wise. Intracellularly Wnts can trigger a number of different pathways, the best understood of which is the canonical/ β -catenin dependent pathway where stabilisation of β -catenin leads to gene expression changes in the responding cell; pivotal components including the Tcf/Lef transcription factors and β -catenin itself. Many other proteins interact at multiple levels in alternative pathways, influencing cellular outputs and this is rendered yet more complex through cross talk between the pathways and other key signals such as BMP (Singh et al., 2018).

A central question is, why are there so many Wnt and Fzd genes in a single organism? Indeed, there are 12 sub-families of Wnt genes conserved across metazoans, with gene loss and duplication in particular lineages (Somorjai et al., 2018). One possibility is that the activities of different members have become segregated during evolution to function in different spatio-temporal contexts in the developing embryo. Here we address this question by making detailed comparisons of comprehensive gene expression patterns using the approach provided by the Mouse Atlas Project which is based on the idea of mapping gene expression and other data onto a series of digital reference models of the mouse at successive stages of development (Davidson and Baldock, 2001). These reference models provide a framework in which the data can be interrogated computationally, integrated in a database with other gene expression data and, importantly, visualised in numerous ways to examine 3D spatial relations in an anatomical context (Armit et al., 2017). Critically, spatial mapping onto an explicit coordinate model embryo enables exploration and analysis of the underlying molecular anatomy unbiased by anatomical interpretation based on histology as has been demonstrated by numbers of projects including the comprehensive Allen Brain Atlas (Lein et al., 2007).

We previously reported comprehensive 3D expression of Wnt and Fzd encoding genes at E11.5 (Theiler stage 19 (Theiler, 1989) (Summerhurst et al., 2008) and of Tcf/Lef transcription factors across time (Vendrell et al., 2009). Here we extend this work using the Mouse Atlas approach to examine and compare RNA expression patterns of genes encoding Wnt ligands (19 genes), Fzd receptors (10 genes), Tcf/Lef transcription factors (4 genes), Secreted Frizzled Related Proteins (Sfrp) (5 genes) and other modulatory proteins, Wif1 and Wise, as well as canonical pathway activity revealed through a reporter mouse line TCF/Lef:H2B-GFP (Ferrer-Vaquer et al., 2010). We studied three key stages when the body plan is being elaborated and various organ systems established: Theiler Stages (TS) 15 (Embryonic day (E) 9.5), 17 (E10.5) and 19 (E11.5). This approach can be used to pose questions not possible in any other way such as asking where no Wnt expression is detected or where specific groups of components are co-expressed or relate to territories of canonical pathway read-out. We set out to test the hypothesis that Wnt and Fzd expression is a mosaic of domains in which only one or a few Wnts and Fzds are expressed in each. Our results also provide insight into the similarity and divergence of expression of different Wnt genes in the mouse, including the deployment of the more recently duplicated paralogous genes and the relation between Wnt pathway component gene expression and canonical pathway activity.

RESULTS

Integrated visualisation of Wnt pathway component gene expression patterns across E9.5 to E11.5 in the mouse embryo.

3D expression patterns for all Wnt, Fzd, Tcf/Lef, Sfrp, Wif1 and Wise genes as well as canonical Wnt pathway readout (Ferrer-Vaquero et al., 2010) were mapped using WlzWarp (Hill et al., 2022) onto reference embryos at E9.5, E10.5 and E11.5 (both data and reference embryos were staged precisely to Theiler Stages 15, 17 and 19 respectively (Theiler, 1989)). All data are available through University of Edinburgh *DataShare* (Murphy et al., 2021a; Murphy et al., 2021b)(<https://doi.org/10.7488/ds/3141>; <https://doi.org/10.7488/ds/3142>) and can also be viewed using an on-line 3D section viewer such as the Mouse Atlas IIP viewer (Armit et al 2015; Husz et al 2012 available at www.emouseatlas.org/WntAnalysis) or downloaded and viewed using ITKSnap (Yushkevich et al., 2006). Examples of mapped and integrated data are shown for Wnt genes (Fig. 1; movies S1-5). The accuracy of mapping (Fig. S1) has enabled an integrated analysis to reveal higher order patterns. Virtual sections through the original, unmapped OPT data have been examined on a gene-by-gene basis to complement this analysis, for example to distinguish epithelial-specific expression. Supplementary movies S1-3 show mapped domains of individual gene expression patterns at E10.5, shown in Fig. 1, while movies S4 and S5 respectively show the integration of three Wnt genes and of all Wnt genes added incrementally.

Fig. 2A shows combined domains for all Wnt ligand genes (red(i)), Fzd receptor genes (green(ii)), and canonical pathway readout from transgenic line TCF/Lef:H2B-GFP (referred to as Tcf/Lef-GFP throughout) (purple (iii)) across stages. Overlaying combined Fzd on Wnt patterns (iv) shows the overlap (yellow). Across stages, combined Fzd domains are more restricted than combined Wnt domains, so that some regions express Wnt genes in the absence of detected Fzd expression (red(iv)). These are extensive, largely ventral and visceral and notably do not overlap with canonical pathway read-out (v). In contrast, domains that show detection of Fzd expression without Wnt expression (green(iv)) are more restricted but with some notable examples such as the anterior telencephalon at E10.5, where Fzd3, 10, 6, 7 and 8 are expressed, the ventral diencephalon at E10.5 and 11.5, and part of the developing limbs at E10.5, contributed to largely by Fzd10. As expected, canonical readout, at any stage, largely fits within the overlap of Fzd and Wnt domains (v), in the dorsal aspects of the main body axis, prominent in the neural tube, and also in the limb, branchial arches and heart. We noted surprising instances where Tcf/Lef-GFP is detected in the absence of concurrently detected Wnt or Fzd expression, notably the nasal epithelium at E11.5, proximal

mesenchyme of the 1st branchial arch at E10.5 and E11.5 (Fig. S2) and regions in the ventral diencephalon at E10.5 and E11.5.

Since all expression domains for each gene at each stage are digitally mapped, it is possible to analyse the domains in the context of the whole embryo or within anatomical subdomains (Baldock et al., 2003; Brune et al., 1999) (Fig. 2B, Table S1). Therefore, one can computationally ask the proportion of the embryo, or of a delineated anatomical structure such as the neural tube, occupied by an expression domain over time. For example, at E10.5, the most broadly expressed Wnt gene in the embryo is Wnt11 (22%), whereas Wnt1, Wnt8a and 8b are very restricted (Fig. 2B; $\leq 1\%$). The extent of expression of Wnt genes is dynamic. Overall expression domains are more restricted at E10.5 compared to E9.5, becoming more expansive again at E11.5 (Fig. 2B), Wnt5a being a striking example (Fig. 2C), but there are notable exceptions, including Wnt11, Wnt6, Wnt3, Wnt2 and Wnt10a, that expand expression domains between E9.5 and E10.5, to become more restricted again at E11.5 (Fig. 2C).

Comprehensive mapping shows territories where no Wnt and Fzd expression is detected (Fig. 3A; see www.emouseatlas.org/WntAnalysis). These territories are largely ventral and visceral and are broadly similar across stages. Territories where expression of a *single* Wnt gene is uniquely detected (Fig. 3B) are mostly represented in ventral, visceral regions, but also in parts of the nervous system; neural tube and diencephalon. These territories are similar between E9.5 and E10.5 but become noticeably more restricted at E11.5 (Fig. 3B). To ask which Wnts are expressed in these single-gene domains, we used parallel co-ordinate visualisation (Moustafa, 2011) across time, showing that a major contributor is Wnt2 at all stages (8, 11 and 17% across stages; representing 49, 54 and 37% of the Wnt2 domains; Table S2). Other major contributors are more dynamic (Fig. 3C). At E9.5 and E10.5, approximately one third of canonical Wnt readout domains are contained within unique Wnt expression territories, becoming about one fifth at E11.5.

Co-expression of multiple Wnt or Fzd genes

At the stages examined, most of the embryo displays the expression of 0 - 2 Wnt or 0 - 2 Fzd genes. However, certain localised regions express a notably large number of Wnt or Fzd genes where the expression of 4 - 11 Wnts or 4 - 8 Fzds maps to each image voxel in the reference model. We refer to the number of genes with expression mapped to a voxel as the *occupancy* of that voxel.

Generally, regions with high occupancy of Wnt or Fzd expression are distinct from one another (Fig. 4), each with one or a few peaks of occupancy (e.g. Fig. 4B E11.5). At all three stages, Wnt occupancy levels 1 and 2 are widely dispersed, but most level 3 Wnt occupancy domains and almost every domain of occupancy 4 and above, contains, or abuts, a region with occupancy 5 or greater (Fig. 4B). In several locations, gradients of Wnt occupancy 4 and above are steep. We have distinguished 'regions of high occupancy' (ROHOs) computationally as territories with occupancy above a certain threshold. For Wnt genes we used five or more (5+) at E9.5 and E11.5 and 4+ at E10.5. For Fzd genes we used 4+ at all three stages. ROHO territories have been analysed in detail (Fig. 4 and Table S3).

In general, each ROHO defined in this way has a consistent location through successive stages (Fig. 4A). The number of Wnt ROHOs is approximately the same at E9.5 and E10.5 and increases at E11.5 when many Wnt ROHOs are more extensive and have higher levels of occupancy (Fig. S4C). Fzd ROHOs also become more extensive between E9.5 and E11.5.

Broadly speaking, Wnt ROHOs and Fzd ROHOs are localised to the same parts of the embryo, but not in all cases (Fig. 4E-I). In particular, many peaks of occupancy in Wnt ROHOs do not coincide with peaks in Fzd ROHOs, even at E11.5 when intersection between Wnt and Fzd ROHOs is maximal (Fig. 4F,G)

The expression of individual Wnts in relation to regions of multiple Wnt expression.

For most Wnt genes, expression is predominantly in domains that intersect Wnt ROHOs (compare Fig. 4C with 4B). However, the existence of Wnt ROHOs is not simply the result of the random intersection of large, unrelated expression domains. The Wnt genes most commonly expressed in ROHOs typically have small to medium-sized domains that individually intersect discrete ROHOs and may extend through the adjacent epithelium or mesenchyme in a manner that appears to be localised around the ROHO (Fig. 4C,D,E). The ROHO-related expression of, for example, Wnt3 at all stages (Fig. 4D) and Wnt7a at E11.5, is largely epithelial. Others, for example Wnt5a, have expression domains that include the epithelium of the ROHO and extend into sub-adjacent mesenchyme (Fig. 4E).

For a few Wnts, e.g. Wnt3 (Fig. 4D), most expression is ROHO-related. However, the majority have both ROHO-related and apparently non-related expression domains. Wnt2 has extensive expression domains in the ventral trunk that display no consistent relation to ROHOs. Wnt6, though expressed

in ROHOs, is expressed quite widely in surface epithelium and does not display convincingly localised expression in ROHOs. However, with the single exception of Wnt16, each Wnt displays at least one instance of local expression in a ROHO at one of the stages we examined.

For a selection of 36 Wnt ROHOs, we examined serial virtual sections to determine which genes have expression domains that intersect any voxel in the ROHO; referred to as the gene set for that ROHO (Table S3 shows ROHO location and gene set; W1-W36, counting ROHOs at each stage as separate). The number of ROHOs in which each Wnt is expressed and the distribution of the number of Wnts per ROHO are shown in Fig. S3A and C. It can be seen in Fig. S3A that Wnt3, Wnt4, Wnt10a or Wnt10b are expressed in almost all the ROHOs we examined. In addition, though their expression is more widespread, Wnt7a or Wnt7b, or both, are expressed in 33/36 ROHOs. Thus, Wnts 3, 4, 7a, 7b, 10a and 10b are commonly expressed in Wnt ROHOs across the three stages (see, for example, Fig. 4D). Wnt3a, could arguably be considered as a member of this common Wnt ROHO set at E9.5 when, strikingly, it is expressed locally and almost specifically in ROHOs.

Apart from the common Wnt ROHO gene set described above, the composition of expression in Wnt ROHOs is dynamic. As development proceeds through the stages we examined, there is a general increase in the number of Wnts expressed in ROHOs (Table S3; Fig. S3C). At E11.5, with only 7 exceptions (Wnt2/2b in W16; Wnt5a/5b in W19; Wnt8a/8b in W13, W14, W21; Wnt9a/9b in W19, W20), each paralogous pair is represented by at least one member in each of the 14 ROHOs examined at that stage. There are some notable instances, for example, Wnt10a and Wnt10b, where the expression of a paralogue at one stage is apparently substituted by its partner at the following stage (Table S3).

The expression of individual Fzds in relation to regions of multiple Fzd expression.

Like the Wnts, most Fzd expression domains intersect Fzd ROHOs examples are Fzds 3, 6, 7, 8 and 10 (Fig. 4L). Unlike Wnt ROHOs, Fzd ROHOs are characterized by the expression of most members of the gene family (Table S3; Fig. S3B). Five of the ten Fzds (3, 6, 7, 8, 10) are expressed in all or nearly all Fzd ROHOs, two (Fzds 1 and 9) are expressed in more than half the Fzd ROHOs we examined and two (Fzds 4 and 5) are expressed in about one third of Fzd ROHOs. 31 of the 39 Fzd ROHOs we examined express 6 or more Fzd genes (Fig. S3D).

Wnt and Fzd ROHOs and canonical Wnt pathway activity

At all three stages, most Wnt ROHOs and Fzd ROHOs show at least partial intersection with Tcf/Lef-GFP activity. In some instances, the correlation is tight (for example the Wnt ROHOs in the distal forelimb and distal hindlimb at E10.5), but in the majority of cases Tcf/Lef-GFP activity, either partly or wholly intersecting the ROHO, extends beyond the ROHO (Fig. 4H,I,J). Some discrete domains of Tcf/Lef-GFP activity, though not intersecting any ROHO, lie in tissue immediately adjacent to one. One example is the isthmus (Table S3: W17, F17) where Tcf/Lef-GFP activity is absent in the flexure but present in the adjacent neural tissue. There are a few instances where Wnt and Fzd ROHOs do not display any apparent correlation with Tcf/Lef-GFP activity, for example in the mandible (Table S3: W2 and F2) at E9.5 (Fig. 4H). However, in these cases, Tcf/Lef-GFP is active at the subsequent stage, intersecting with the corresponding ROHO (Fig. 4I).

Comparison of patterns: similarity and divergence of paralogous pairs of Wnt genes

We previously compared the expression of four pairs of Wnt paralogues (Wnt2, Wnt5, Wnt7 and Wnt8) between mouse and chick embryos (Martin et al., 2012). Here we compare seven pairs of paralogues (Wnt1, 3, 5, 7, 8, 9, 10) for overall similarity and divergence of expression in the mouse. Fig. 5 compares the whole embryo expression patterns at E10.5 and Table 1 shows the Jaccard similarity indices (JI) for each pair in the whole embryo (Jaccard Index = volume of intersection/volume of union of the two domains). Wnt7a and Wnt7b show the greatest similarity of any pair of Wnt genes across all stages with extensive overlap in the CNS (Table 1; Fig. 5D; Table S4). Their expression patterns however show complementarity especially in the dorsal and ventral aspects of the forebrain (Fig. 5D). Wnt7a is more widely expressed than Wnt7b in the neural tube and limb. The Wnt3 paralogues also show extensive similarity with the second highest JI at E9.5 among any Wnt gene pair and a high score across stages. Although distinct, extensive overlap in the midbrain is clear (Fig. 5B). There is also overlap in the posterior neural tube. The Wnt10 paralogues are distinct at E9.5 (Wnt10b expression is extensive at this stage and more similar to other patterns) and most similar to each other at E10.5 and E11.5, particularly in the limbs, although the level of similarity is low for E11.5 (0.06). Wnt5 and Wnt9 paralogues show increased expression similarity over time, while Wnt5 genes become more divergent from other patterns in general. Wnt2 and Wnt8 paralogues show most distinct patterns with weaker similarity indices than most other pairs of non-paralogous Wnt genes (Table S4).

Comparison of patterns: all gene expression patterns and canonical pathway activity

The expression domains of all genes and canonical readout were examined for overlap using parallel-coordinate analysis, JI similarity (Table S4) and visual comparison. Fig. 6A shows striking similarity between where 3+ Wnts are co-expressed and canonical pathway readout, compared to where 0 or unique genes are expressed. Fig. 6A also illustrates each component gene expression pattern at E11.5. Table S4 shows the JI for each pair of genes. Plotting pairwise JI across stages (Fig. 6C), it is clear that Wnt gene family expression patterns generally become more similar to each other over time, with some notable exceptions (Wnt1, Wnt6, and Wnt10). This is also the case when comparing across Wnt and Fzd gene families. For example, while 50% of the Wnt16 expression domain lies outside any Fzd expression domain at E9.5, this drops to 13% at later stages. This is also reflected in the proportion of any pattern that is uniquely expressed (Table S2). Wnt gene similarity indices were plotted as networks to compare the relationships between expression patterns across stages. For each stage, we plotted network graphs in which genes are presented as nodes connected by “edges” with a line thickness that represents the similarity (JI) between expression patterns. Fig. 6B illustrates networks for the 15 Wnt genes that display the most similar patterns to other Wnts. The patterns can be divided into 3 groups:

Group 1: Core set of genes with expression patterns that show high JIs when paired (Fig.6Bi; blue circled). This includes Wnt7 and Wnt3 paralogues, and Wnt4. Wnt1 is also included at E9.5 and E11.5. These expression patterns are most similar to canonical readout (Fig. 6A; Table S4). Wnt4 changes somewhat over time; while consistently similar to Wnts3, 7 and Wnt5a, it becomes more similar also to other patterns (Wnt8a, Wnt16, Wnt9a, Wnt2b) at E11.5, due largely to a new territory of forebrain expression (Fig. 6B).

Group 2: Wnt11, Wnt16 and Wnt2 show low similarity across stages (Fig. 6Bi; red circled) and are among the genes with the largest proportion of unique expression (Table S2; Fig. 3C). Visual analysis shows the patterns are distinct from canonical read-out (Fig. 6A). Both Wnt11 and Wnt16 show low similarity generally at E9.5 with some similarity to each other by E10.5 (0.04). Both begin to be expressed in the brain at E11.5 driving increased similarity to other patterns at that stage; however, while Wnt16 shares brain expression domains with more commonly expressed Wnt genes it is most similar to Wnt2, Wnt9b and Wnt11 in the trunk.

Group 3: The remaining gene expression patterns (Fig. 6Bi, uncircled) show intermediate similarity that can vary across stages; at some stages they may be more similar to Group 1 genes. These include Wnt5, Wnt8, Wnt9 and Wnt10 paralogues, and Wnt2b. It is striking that both Wnt8a and

Wnt8b patterns are most similar to Wnt9a at E10.5 although they show very low similarity to each other; Wnt9a shares different aspects of both patterns. Wnts 9a and 9b become more similar to each other and share expression territories most with Wnt16 at E11.5. Wnt2b becomes more typical of Group 1 patterns at E11.5. At E9.5 Wnt5a shows strong similarity to Wnt7 paralogues while Wnt5b shows an intermediate pattern; however, Wnt5b expression becomes more distinct from other Wnt patterns with time; at E11.5 it shows some similarity with Group 1 genes largely through neural expression while it intersects Wnt16 and Wnt2 in the trunk. Wnt10b expression is extensive at E9.5 driving more similarity with Group 1 genes, but the pattern is overall very distinct. At E10.5 Wnt10a becomes more similar to Group 1, largely due to midbrain expression while Wnt10b is more similar to Wnt2 and Wnt16.

The expression pattern of each Wnt gene generally comprises several sub-domains that are shared with some other Wnts but absent or much reduced in others. Thus, for example, at E10.5, Wnt expression in the dorso-lateral neuro-epithelium of the future telencephalon, in the anterior neural tube, mandible, branchial arches (grooves and pouches) and proximal limb comprises different combinations of genes. We examined the pattern similarities represented by the lines connecting pairs of genes in the network graph (Fig.6Bi (edges)) from this perspective. Fig. 6Bii presents a visual picture of edges in the network graph: in some instances, multiple connections to the same gene in the network reflect similar, though not identical, sets of intersecting expression domains (e.g. Wnt3a to Wnt10a and to Wnt4 at E10.5), whereas, in other instances, different connections to the same gene reflect different combinations of intersecting domains (e.g. Wnt4 to Wnt3a and to Wnt3 at E10.5). Fig. 6Bii strikingly reveals that a domain centred on the midbrain is shared by all group 1 genes.

Pair-wise comparison reveals that Fzd gene expression falls broadly into two pattern classes. Class 1; Fzd 3, 6, 7, 8, 9, 10, and to a lesser extent Fzd1, show general overlap and similarity of expression across stages (Fzd2 is not detected at any stage, Fzd5 is not detected and Fzd1 very little expression at E9.5; Fzd9 expression is restricted largely to the brain) (Fig. 6D). Class 1 patterns also show general overlap with canonical pathway readout (at E11.5, Fzd versus readout JIs range from 0.26 (Fzd10) to 0.01 (Fzd9)), with extensive commonality with expression of the Tcf/Lef transcription factors and Sfrp modulators. In contrast, Class 2 patterns, Fzd4 and Fzd5, show much less similarity with readout (0.057 for Fzd4 and 0.025 Fzd5), each with distinct patterns. These different groups of Fzd patterns also overlap with different Wnt expression patterns, although the individual Wnts involved are dynamic over time. While Class 1 Fzd patterns predominantly show similarity with Wnt Group 1,

Fzd4 and Fzd5 both show greatest similarity to Wnt9a and Wnt8a at E10.5, with increased similarity with Wnt16 (0.124 and 0.149) and Wnt11 (0.059 and 0.12) at E11.5.

Among Tcf-Lef transcription factor patterns, Tcf7 and Lef1 are most similar and Tcf7l2 is the most divergent pattern across stages (Fig. 6D; Table S4). Sfrp gene expression patterns are dynamic, with Sfrp4 more divergent at E10.5 but more similar, particularly to Sfrp1 by E11.5 (change from 0.15 to 0.33 JI) (Fig. 6D) (note Sfrp5 expression was not detected). Sfrp1-4 patterns were also analysed visually for co-expression (Fig. 4M,N). Regions with co-expression of 3 and 4 Sfrp genes are generally well-defined and discrete. At E10.5, these regions rarely coincide with Wnt ROHOs; e.g. in the core mesenchyme and distal epithelium of the developing branchial arches (Fig. 4M). However, by E11.5, domains of multiple Sfrp gene expression intersect the expanding Wnt ROHOs, for example within, or close to the surface epithelium in the developing face and limbs (Fig. 4N).

The Fzds show some interesting relationships to Sfrp patterns, but the Wnts are more complex and do not show consistent general relations with Sfrps. For example, at E10.5, the group of Fzds 6, 7, 8 and 10 show similarities of expression to Sfrp2 in the face while Fzds 4, 5 and 9 patterns display no apparent relation to Sfrp2 expression. At E11.5, Sfrp2 intersects Fzd7 expression in interesting patterns in the face, limb and trunk, while Sfrp4 intersects Fzd7 in an interesting pattern in the limb.

Detailed analysis of integrated expression patterns in the ventral diencephalon

Using the resource provided here novel insights can be gleaned through focused analysis of any region of the embryo and used to build testable hypotheses. For example, examining the ventral diencephalon (VD) at E10.5 revealed a striking complementarity between Shh and canonical Wnt readout (Fig. 7A-D). Tcf/Lef-GFP showed a gradient of expression through the midline of the VD that was strongest in the peduncular hypothalamus and the terminal hypothalamus caudal to the infundibulum. In particular, 3D rendered images of mapped data show that the Shh expression domain surrounds the Tcf/Lef-GFP domain (Fig. 7C).

We asked what Wnt and Fzd expression combinations might drive expression of the Tcf/Lef-GFP reporter in the VD by digitally segmenting (Baldock et al., 2003; Brune et al., 1999) the VD anatomical domain in the E10.5 reference model and examining the mapped expression of genes in the Wnt signalling system using parallel co-ordinate analysis. We asked which genes are detected a) where Tcf/Lef-GFP is active and b) where Shh is expressed (Fig. S4). We then confirmed expression of these Wnt and Fzd genes in the VD neuroepithelium and Rathke's pouch through visualisation of

mid-sagittal sections of both mapped and original 3D OPT data. Visual examination revealed that the region positive for canonical Wnt-readout shows limited detection of Wnt and Fzd expression at E10.5 (Fig. 7Ei-iii). Indeed, most of the region shows zero Wnt detection and there are only restricted regions of single Wnt genes; Wnt2, Wnt4, Wnt7b and Wnt1 within the territory (Fig. 7Ei). Similarly, much of the region shows no detectable expression of Fzd genes; only Fzd7, Fzd3 and Fzd1 are expressed in restricted sub-regions (Fig. 7Eiii). In contrast, rostrally and caudally, where Shh is detected, multiple Wnts and Fzds are expressed (Fig. 7Eiv and v). For other members of the Wnt signalling system only Sfrp4 is expressed in the cephalic flexure and in the caudal VD but not throughout the rostral VD where the pathway is active (Fig. 7E vi). Among Tcf/Lef transcription factors, there is extensive expression of Tcf7l1 and Tcf7l2 whereas Lef1 and Tcf7 are restricted to the caudal VD (Fig. 7Evii). Ror2 is expressed, most strongly in the caudal VD (Fig. S4). In summary, canonical readout is seen in the VD where Tcf/Lef transcription factors are expressed and Sfrp expression is restricted, but where, in a substantial part of the region, no Wnt or Fzd expression was detected. Shh is expressed where no canonical output is detected.

A day later, at E11.5, the region still has limited Wnt and Fzd gene expression while canonical readout is restricted more caudally (Fig. 7F). To investigate if the activity at E10.5 could be due to earlier expression of Wnts and Fzds we examined data at E9.5 which showed a single Wnt gene, Wnt7A, and two Fzd genes (5 and 7) expressed (Fig. 7G). While we detected no canonical activity at E9.5, these pathway components could be involved in triggering later activity.

DISCUSSION

Wnt signalling is one of the most studied sets of biological pathways, yet the challenge to understand the basis of spatial and temporal control of its biological outputs during development remains. Decades of work has described the expression of individual or small sets of genes in the vertebrate system, but the picture that emerges is patchy and driven by the focus of diverse studies. Here we have used the Mouse Atlas approach to capture comprehensively the expression patterns of all Wnt genes, their Fzd receptors, Sfrp modulators, Tcf/Lef transcription factors as well as other interacting factors in mouse embryos in 3D over the developmental period when the patterning of different organ rudiments is being elaborated. Mapping the expression of different genes to common 3D digital models of embryos at each stage enabled an integrated spatio-temporal analysis of the patterns and comparison to a reporter (Ferrer-Vaquer et al., 2010) that reveals activation of one of several pathway outputs, the canonical pathway. This study provides insight into a level of

organisation of the patterns not previously apparent, as well as presenting a resource that can be utilised further by the research community.

Our comprehensive approach indicated that the territories where no Wnt and no Fzd expression is detected across the three stages are largely ventral and visceral. Given the dynamism of the patterns, it is possible that a region where there is no detected expression at one stage might show expression at another, however there is clearly some consistency in the regions that show no detected expression across the three stages assessed here. Territories where the expression of only one Wnt gene was detected are also predominantly ventral, in particular expression of Wnt2 across stages and Wnt11 at E10.5 (Fig. 3C). Both genes show very divergent expression in our cross-pattern analysis (Fig. 6B) pointing to possible unique roles. They show mutant phenotypes in the placenta, kidneys and lungs consistent with these patterns (Goss et al., 2009; Majumdar et al., 2003; Monkley et al., 1996). Domains where only one Wnt is expressed may also represent evolutionary diversification involving changes in gene regulation, more recently evolved territories of expression and neofunctionalization (Ohno S, 1970). By contrast, those domains with expression of multiple genes in all families are in dorsal and lateral regions, particularly the central nervous system, limbs, flank and face, consistent with the primary body axis being determined along the dorsal midline (for example (Arraf et al., 2016).

Not surprisingly, regions of the embryo show extensive overlap in domains of Wnt and Fzd expression and canonical read-out. In relation to the proximity of Wnt mRNA signal to sites expressing Fzd receptor RNA or canonical readout, it is worth noting that in regions where Vangl2 is co-expressed (largely the nervous system) active Wnt protein may be present in long cytoneme processes extending from Wnt-expressing cells so that the signaling activity may be distant from cell bodies expressing Wnt mRNA (Brunt et al., 2021)

To address the question why there are so many Wnt and Fzd genes in a single organism, we have examined the hypothesis that Wnt and Fzd expression is a mosaic of domains, each expressing only one or a few members of these families. Our results are not consistent with this hypothesis. Some anatomical regions show the expression of one or a few Wnts co-expressed, similar to what would be expected from this hypothesis. But there are many regions co-expressing strikingly large numbers of Wnts and Fzds. The focus of the question thus shifts to why are so many Wnts and Fzds co-expressed in these regions?

A striking finding is the co-expression of a large fraction of all Wnt or Fzd genes in localised regions of the embryo (termed ROHOs). These regions may reflect regulatory “hot spots” for the gene families. Some coincide with known Wnt signalling centres such as the isthmus and the cortical hem but others are novel and have not been previously detected, for example the flank anterior to the forelimb (W5 in Table S4) and the ventral aspect where the forelimb meets the flank (W8 in Table S4). It is important to note that generally each gene has a distinctive expression pattern extending beyond the ROHO, often including domains unconnected to ROHOs. The intersection of patterns in ROHOs generally suggests spatio-temporal regulation centred on a small region of tissue. These observations open an avenue to investigating the signalling characteristics of these regions and their importance in patterning.

Asking how ROHOs relate to canonical pathway activity, there is generally correspondence between Wnt and Fzd ROHOs and pathway readout, but this is neither universal nor precise. The respective peaks of Wnt and Fzd ROHOs are usually offset. The same is true of regions of Tcf/Lef-GFP reporter activity. Even taking account of the possible involvement of cytonemes in signalling, this suggests that it is not simply the additive effect of multiple Wnt genes that activates the pathway; the relationship is more complex reflecting the full regulatory landscape. Indeed, canonical signalling is not restricted to Wnt and Fzd ROHOs. We have quantified the extent of each expression domain and compared the territories where different numbers of Wnt genes are co-expressed with canonical Wnt readout showing that 33% of readout falls within regions of unique Wnt gene expression at E9.5 and E10.5. We also found canonical Wnt pathway readout in the absence of any detectable concurrent Wnt or Fzd gene expression (e.g. in nasal epithelium at E11.5 and the ventral diencephalon at E10.5 and E11.5). In the case of the VD, earlier (E9.5) expression of individual Wnt and Fzd genes could account for the later activity.

Another striking feature of all Wnt patterns is that they generally become more similar over the developmental time period covered (Fig. 6C); also reflected in the increased overlap of genes in ROHOs over time. Pairwise comparisons of similarity between expression patterns using the Jaccard Index (Table S4) provides a view of the deployment of Wnt function that complements the co-expression analysis. Network analysis of pairwise comparisons (Fig. 6B) revealed three groupings of patterns. The first (Group 1) are similar across stages and often associated with regions of canonical pathway activity and Wnt ROHOs (Table S4; expression of Wnts 3, 7 and 4 occurs in >30/36 ROHOs analysed) while the second (Group 2) are less associated with canonical activity and include the genes most expressed in unique territories and in ventral and visceral domains (Wnts 2 and 11). A third group are intermediate and/or change their similarities over time; e.g. Wnt10a is very closely

related to Group 1 patterns at E10.5 but dramatically less so at other stages. Group 1 expression patterns might lie closer to an ancestral pattern aligned with the primary body axis, while other patterns are more divergent and associated with recently added Wnt system functions: e.g. Wnt2 association with placental development and Wnt11 with kidney development. The predominant elements in the similarity between group 1 patterns lie within the CNS including the dorsal midbrain, the cortical hem in the forebrain and the dorsal neural tube. Interestingly, further analysis of the similarity between Group 1 patterns (Fig. 6Bii) suggests that the expression of each of these genes comprises combinations of subdomains shared with some but not all members of the set indicative of modular regulation.

Turning to the question why so many Wnts and Fzds are co-expressed in localised regions, there are three non-exclusive possibilities:

- A. Convergent evolution of independent family members to satisfy a functional requirement for the expression of multiple genes, e.g. a threshold for Wnt ligand concentration.
- B. Conserved regulation of Wnts and Fzds, either active or passive.
- C. The existence of spatio-temporal regulatory control that spans the family, i.e. a form of “meta-regulation” of the family. This raises the possibility that there exists a level of regulation, hitherto unknown, that directs the expression of the Wnts as a suite, and similarly for Fzds. One possibility, for example, would be positive feedback regulation across the gene family.

We envisage that these possibilities apply not to the entire expression pattern of any gene, but rather to independently regulated sub-domains of expression. Indeed, there is no obvious simple relation between the net similarity of expression of pairs of genes represented in Figure 6Bi and either their phylogenetic relationships based on DNA sequence (Somorjai et al 2018), or certain widely conserved, tight chromosomal linkages (between Wnts1 and 10b, 6 and 10a, 3a and 9a, 3 and 9b (Ensemble genome browser <https://www.ensembl.org/index.html>). The potential for evolutionary conservation and shuffling of cis or trans regulatory modules, perhaps controlling different parts of each pattern (as for example, in Fig. 6Bii), may be a fruitful area for future investigation (Marlétaz et al., 2018). Interestingly, Wnt expression studies in *Amphioxus*, which has 13 Wnt genes, also shows regions where multiple Wnts are expressed, for example posterior nested expression domains (Somorjai et al., 2018). This suggests that spatio-temporal intersection is not unique to the more complex gene family in the mouse. Evolutionary studies comparing *Amphioxus* and the tunicate *Oikopleura dioica* have suggested three modes of evolutionary change in the Wnt

gene family namely, conservation of function, function shuffling and gene loss (Martí-Solans et al., 2021). It is possible that the co-expression of subdomains of different Wnts in the mouse reflects the operation of a conserved ancestral regulation, though not necessarily conservation of precise gene function, across different Wnts.

We previously compared the expression of four pairs of Wnt paralogues within and between mouse and chick embryos (Wnt2, Wnt5, Wnt7 and Wnt8) (Martin et al., 2012) showing evidence of greater divergence between subgroup paralogues than the respective orthologues, consistent with conserved subfunctionalisation/neofunctionalisation in the common vertebrate ancestor. Here we compare all seven paralogue gene pairs reinforcing earlier observations and adding new insight. The Jaccard Index shows that Wnt7 and Wnt3 paralogues are most similar of all Wnt pairwise patterns (Table 1 and Table S4), yet the patterns are distinct, often complementary, in the same anatomical region. Contrastingly, Wnt2 and Wnt8 paralogues have diverged enormously in their expression characteristics, across all stages. Wnt10 genes present an interesting case where they appear to “swap” territories over time; especially evident in ROHO analysis where the same ROHO switches between expressing Wnt10a and Wnt10b (Table S3). These results add to our understanding of how paralogues arising by duplication of highly conserved genes evolve individually, sometimes maintaining aspects of their regulatory inputs while adjusting precise expression domains within that territory, and/or by acquiring new territories of expression. These findings present interesting contrasting cases (e.g. Wnt7 vs Wnt2 respectively) to dissect the regulatory inputs for each gene pair to fully understand the regulatory changes involved.

In addition to the global analysis described above, our results can be used with a focus on individual organs and as a resource to complement hypothesis-driven approaches. As a case study, we analysed the ventral diencephalon (VD) in some detail. The VD goes on to form the hypothalamus and the neurohypophysis that innervates the oral ectoderm-derived pituitary (adenohypophysis) through the infundibular stalk; together these components form the hypothalamic-pituitary axis, of major importance in homeostasis. Initially using Shh as a marker gene, we immediately noticed a striking complementary pattern between Shh and the Tcf/Lef-GFP reporter (Fig. 7), suggestive of a repressive relationship between canonical Wnt signalling and Shh expression in this territory. Indeed Osmundsen et al. (Camper et al., 2017; Osmundsen et al., 2017) have demonstrated that rostral expansion of beta-catenin activity leads to coincident loss of Shh expression, elegantly demonstrating our original conjecture from visual analysis.

We further suggest a role for Wnt/Beta-catenin signalling in development of the neurohypophysis, in particular the evaginating infundibulum, and reveal Wnt signalling pathway gene expression patterns that could contribute to this important regulatory output. By digitally dissecting the territories that express Shh and those which show Tcf/Lef-GFP activity, coupled with parallel-coordinates visualisation, we could find potential regulatory inputs to the observed Tcf/Lef-GFP output; i.e. the cocktail of Wnts, Fzds and other regulatory components that are expressed in the region. Surprisingly few Wnts and Fzds are expressed in the region of Tcf/Lef-GFP activity, and none throughout the region at E10.5 and 11.5 whereas very many genes are expressed in the Shh +ve territory where Tcf/Lef-GFP is not active. However, at the earlier stage of E9.5 Wnt7a and Fzd5 and 7 are expressed in the region that later becomes Tcf/Lef-GFP. This cautions against drawing conclusions about pathway activity based on component gene expression patterns alone.

To further explore the ventral diencephalon, making use of the Mouse Atlas EMAGE database, we carried out a spatial query for genes with similar patterns to Shh and Tcf/Lef-GFP. This identified *Vax1* with a complementary pattern to Tcf/Lef-GFP. *Vax* genes are of particular interest since they are known to inhibit canonical Wnt signalling through activation of an internal promoter transcribing a dominant-negative isoform of Tcf712 (Vacik et al., 2011). Furthermore they are dependent on Shh signalling (Zhao et al., 2010) consistent with a mutually repressive relationship between Shh and Wnt signalling through expression of *Vax1*. We hypothesise that this Shh-dependent inhibition of Wnt/Beta-catenin signalling in the rostral VD is necessary to limit the pituitary forming territory, consistent with ectopic pituitary formation in *Vax1*-deficient mice (Bharti et al., 2011)

The data reported here can be used to help direct future investigation of the global regulation and function of Wnt and Fzd family genes. In particular, it will be interesting to investigate the effects of manipulating individual genes on the expression and function of co-expressed members of the family. By providing a means to directly visualise comparisons between data in 3D and to incorporate retrospective and future data, the approach provides an opportunity to complement the data reported here with mutational and high resolution, multiplex approaches (Lohoff et al., 2021).

EXPERIMENTAL PROCEDURES

Expression patterns were generated by *in situ* hybridisation as previously described (Summerhurst et al., 2008) for *Sfrp1-4*, *Ror2*, *Wif1*, and *Wise*, including previously reported Wnts, Fzds and Tcf/Lef genes. The cDNA sequences used for generation of RNA probes are detailed in Supplementary Table 5. Readout of the canonical pathway was revealed using GFP expression (both RNA in situ and anti-

GFP immunofluorescence [Invitrogen A11122 1:200] in a previously characterised transgenic mouse line (Ferrer-Vaquer et al., 2010).

3D imaging was carried out using Optical Projection Tomography (OPT) as previously described (Summerhurst et al., 2008).

Mouse embryos are referred to by embryonic day (E), however, embryos analysed were staged according to Theiler criteria (Theiler, 1989) to Stages 15, 17 and 19, referred as E9.5, E10.5 and E11.5 respectively. Expression patterns are submitted to the Edinburgh Mouse Atlas of Gene Expression (EMAGE; IDs noted on Table S5), available at <https://www.emouseatlas.org/emage/home.php>. Patterns can also be viewed openly at <https://www.tcd.ie/Zoology/research/groups/murphy/WntPathway/>

Mapping of gene expression data:

3D gene and reporter patterns were mapped onto reference embryos at each stage using a manual image-editing tool WlzWarp (Hill et al., 2022). This uses *Constrained Distance Transform* (Hill and Baldock, 2015) which can deliver the complex non-linear transforms required for the variable shape and pose of mouse embryos. WlzWarp is an open-source tool (github.com/ma-tech) and provides interactive non-linear spatial mapping of 3D image data. This has been used for mapping significant volumes of gene-expression data and tested by mapping multiple images of the same gene from independent samples (Hill et al., 2022). The process is straightforward with the key required competence being an understanding of the biology and anatomy rather technical IT expertise. More detail is provided by Hill *et al*, 2022, but the mappings for this data required operator time per embryo of about 60 minutes. Fig. 1 illustrates mapping examples. Mapping accuracy was assessed for each gene by comparing virtual sections of original 3D data (unmapped) against the mapped data (Fig. S1) showing good fidelity in most cases, reduced when mapping surface (ectodermal) expression (Fig. S1F).

Analysis of integrated data:

Primary checking and visual analysis of 3D expression data and mapped patterns used open-source tools MAPaint and MA3DView (github.com/ma-tech). For visualisation of mapped patterns we used the IIP Viewer providing access to the data within a standard web-browser (Armit et al., 2015; Husz

et al., 2012). The IIPViewer allows the user interactive selection of arbitrary section views through the mouse embryo and an overlay of all or any combination of the gene-expression patterns (available at www.emouseatlas.org/WntAnalysis). For convenience we have included many of the derived patterns of multiple gene-occupancy including regions where a single gene within a gene family is expressed.

In addition to this section-based visualization we provide a full-3D rendered view using the “point-cloud” approach which delivers a volumetric style view of the entire pattern. Again, viewing any gene-combination can be interactively selected including the entire gene-set. The IIPViewer and point-cloud software and tools for generating the associated data are all open-source from the GitHub ma-tech repositories.

Analysis of mapped expression regions was undertaken using bespoke software tools based on the Woolz image-processing system (Piper and Rutovitz, 1985); github.com/ma-tech/woolz). The tools are csh-scripts that can be executed on any Unix-based system (e.g. Linux, Mac OSX) and generate all of the data values used for the downstream analysis. Specifically they generate:

1. Tables of pair-wise intersection volumes as a count of the number of voxels in common between the two patterns normalised either by the test-pattern volume (row-normalised) or the target pattern volume (column normalised). The overall volumes are provided to enable calculation of absolute volume values and using the voxel resolution these can be converted to real-space (μm^3) values;
2. Tables of pair-wise similarity values using the Jaccard index (Levandowsky and Winter, 1971) based on the voxel set intersection and union volumes;
3. Volumetric domains of gene-occupancy which for a given gene set (e.g. Wnt) are calculated from the gene-count, i.e. number of genes expressed at every voxel location within the embryo. This occupancy “image” is then thresholded to define regions where for example there are 5 or more Wnts expressed at the same location. This can then be further analysed to reveal which genes are expressed within that region. Such occupancy data was used to reveal the regions of high-occupancy (ROHO) as well as regions of single gene occupancy where there is no overlapping expression within the gene-family;
4. Re-formatted data for visualisation using the IIPViewer, point-cloud viewer and for the parallel-coordinate visual analysis using D3.js (d3js.org) Javascript visualisation library;
5. Re-formatted data for network analysis and input to CytoScape.

All data required for these views are provided in a series of datasets held at the University of Edinburgh public data repository for Wnt Pathway Analysis (Murphy et al., 2021a; Murphy et al., 2021b) <https://doi.org/10.7488/ds/3141>; <https://doi.org/10.7488/ds/3142>). In addition, links to the parallel-coordinate views we have used are available at www.emouseatlas.org/WntAnalysis for convenience.

The network analysis software *igraph* (Csardi G and Nepusz T, 2006) igraph.org/, was used to construct networks according to the Jaccard indices of similarity across a variety of threshold levels across stages. The threshold level that showed the top 15 most similar genes at each stage was selected for detailed comparison and network visualisation using cytoscape (Shannon et al., 2003); cytoscape.org) with the network layout unchanged.

Acknowledgements:

We thank Peter Hohenstein and Anna Thornburn for providing Tcf-Lef-GFP embryos used in this study. We thank Yiwen Sun for contribution to mapping of the E9.5 stage. Several students contributed to testing analysis of mapped data, especially Daniel Darby, Jessica Maddock and Cliodhna Smyth. Martina Redmond and Somantha Killion-Connolly assisted with generation of gene expression data. This work was supported by Science Foundation Ireland (Programme Award 02/IN1/B267) and the Irish Research Council.

References

- Armit, C., Richardson, L., Hill, B., Yang, Y. and Baldock, R. A. (2015). eMouseAtlas informatics: embryo atlas and gene expression database. *Mamm Genome* **26**, 431-440.
- Armit, C., Richardson, L., Venkataraman, S., Graham, L., Burton, N., Hill, B., Yang, Y. and Baldock, R. A. (2017). eMouseAtlas: An atlas-based resource for understanding mammalian embryogenesis. *Dev Biol* **423**, 1-11.
- Arraf, A. A., Yelin, R., Reshef, I., Kispert, A. and Schultheiss, T. M. (2016). Establishment of the Visceral Embryonic Midline Is a Dynamic Process that Requires Bilaterally Symmetric BMP Signaling. *Dev Cell* **37**, 571-580.
- Baldock, R. A., Bard, J. B., Burger, A., Burton, N., Christiansen, J., Feng, G., Hill, B., Houghton, D., Kaufman, M., Rao, J., et al. (2003). EMAP and EMAGE: a framework for understanding spatially organized data. *Neuroinformatics* **1**, 309-325.
- Bharti, K., Gasper, M., Bertuzzi, S. and Arnheiter, H. (2011). Lack of the ventral anterior homeodomain transcription factor VAX1 leads to induction of a second pituitary. *Development* **138**, 873-878.

- Brune, R. M., Bard, J. B., Dubreuil, C., Guest, E., Hill, W., Kaufman, M., Stark, M., Davidson, D. and Baldock, R. A.** (1999). A three-dimensional model of the mouse at embryonic day 9. *Dev Biol* **216**, 457-468.
- Brunt, L., Greicius, G., Rogers, S., Evans, B. D., Virshup, D. M., Wedgwood, K. C. A. and Scholpp, S.** (2021). Vangl2 promotes the formation of long cytonemes to enable distant Wnt/ β -catenin signaling. *Nat Commun* **12**, 2058.
- Camper, S. A., Daly, A. Z., Stallings, C. E. and Ellsworth, B. S.** (2017). Hypothalamic β -Catenin Is Essential for FGF8-Mediated Anterior Pituitary Growth: Links to Human Disease. *Endocrinology* **158**, 3322-3324.
- Clevers, H., Loh, K. M. and Nusse, R.** (2014). Stem cell signaling. An integral program for tissue renewal and regeneration: Wnt signaling and stem cell control. *Science* **346**, 1248012.
- Csardi G and Nepusz T** (2006). The igraph software package for complex network research. *InterJournal Complex Systems* **1695**.
- Davidson, D. and Baldock, R.** (2001). Bioinformatics beyond sequence: mapping gene function in the embryo. *Nat Rev Genet* **2**, 409-417.
- Ferrer-Vaquer, A., Piliszek, A., Tian, G., Aho, R. J., Dufort, D. and Hadjantonakis, A. K.** (2010). A sensitive and bright single-cell resolution live imaging reporter of Wnt/ β -catenin signaling in the mouse. *BMC Dev Biol* **10**, 121.
- Goss, A. M., Tian, Y., Tsukiyama, T., Cohen, E. D., Zhou, D., Lu, M. M., Yamaguchi, T. P. and Morrissey, E. E.** (2009). Wnt2/2b and beta-catenin signaling are necessary and sufficient to specify lung progenitors in the foregut. *Dev Cell* **17**, 290-298.
- Hill, B. and Baldock, R. A.** (2015). Constrained distance transforms for spatial atlas registration. *BMC Bioinformatics* **16**, 90.
- Hill, B., Husz, Z., Armit, C., Davidson, D. R., Murphy, P. and Baldock, R. A.** (2022). WlzWarp: An Open-Source Tool for Complex Alignment of Spatial Data. *bioRxiv*, 2022.2002.2011.480105.
- Holstein, T. W.** (2012). The evolution of the Wnt pathway. *Cold Spring Harb Perspect Biol* **4**, a007922.
- Husz, Z. L., Burton, N., Hill, B., Milyaev, N. and Baldock, R. A.** (2012). Web tools for large-scale 3D biological images and atlases. *BMC Bioinformatics* **13**, 122.
- Itoh, N. and Ornitz, D. M.** (2011). Fibroblast growth factors: from molecular evolution to roles in development, metabolism and disease. *J Biochem* **149**, 121-130.
- Lein, E. S., Hawrylycz, M. J., Ao, N., Ayres, M., Bensinger, A., Bernard, A., Boe, A. F., Boguski, M. S., Brockway, K. S., Byrnes, E. J., et al.** (2007). Genome-wide atlas of gene expression in the adult mouse brain. *Nature* **445**, 168-176.
- Levandowsky, M. and Winter, D.** (1971). Distance between Sets. *Nature* **234**, 34-35.
- Loh, K. M., van Amerongen, R. and Nusse, R.** (2016). Generating Cellular Diversity and Spatial Form: Wnt Signaling and the Evolution of Multicellular Animals. *Dev Cell* **38**, 643-655.
- Lohoff, T., Ghazanfar, S., Missarova, A., Koulena, N., Pierson, N., Griffiths, J. A., Bardot, E. S., Eng, C. L., Tyser, R. C. V., Argelaguet, R., et al.** (2021). Integration of spatial and single-cell transcriptomic data elucidates mouse organogenesis. *Nat Biotechnol*.
- Majumdar, A., Vainio, S., Kispert, A., McMahon, J. and McMahon, A. P.** (2003). Wnt11 and Ret/Gdnf pathways cooperate in regulating ureteric branching during metanephric kidney development. *Development* **130**, 3175-3185.
- Marlétaz, F., Firbas, P. N., Maeso, I., Tena, J. J., Bogdanovic, O., Perry, M., Wyatt, C. D. R., de la Calle-Mustienes, E., Bertrand, S., Burguera, D., et al.** (2018). Amphioxus functional genomics and the origins of vertebrate gene regulation. *Nature* **564**, 64-70.

- Martí-Solans, J., Godoy-Marín, H., Diaz-Gracia, M., Onuma, T. A., Nishida, H., Albalat, R. and Cañestro, C.** (2021). Massive Gene Loss and Function Shuffling in Appendicularians Stretch the Boundaries of Chordate Wnt Family Evolution. *Front Cell Dev Biol* **9**, 700827.
- Martin, A., Maher, S., Summerhurst, K., Davidson, D. and Murphy, P.** (2012). Differential deployment of paralogous Wnt genes in the mouse and chick embryo during development. *Evol Dev* **14**, 178-195.
- Monkley, S. J., Delaney, S. J., Pennisi, D. J., Christiansen, J. H. and Wainwright, B. J.** (1996). Targeted disruption of the Wnt2 gene results in placentation defects. *Development* **122**, 3343-3353.
- Moroz, L. L., Kocot, K. M., Citarella, M. R., Dosung, S., Norekian, T. P., Povolotskaya, I. S., Grigorenko, A. P., Dailey, C., Berezikov, E., Buckley, K. M., et al.** (2014). The ctenophore genome and the evolutionary origins of neural systems. *Nature* **510**, 109-114.
- Moustafa, R. E.** (2011). Parallel coordinate and parallel coordinate density plots. *WIRES COMPUTATIONAL STATISTICS* **3**, 134-148.
- Murphy, P., Summerhurst, K., Brady, G., Vendrell, V., Frankel, P., Redmond, M., Lillion-Connolly, S., Armit, C., Hill, B., Venkatarman, S., et al.** (2021a). Wnt Pathway Analysis mapped gene-expression point-cloud data. *Edinburgh DataShare*, 2021.2009.2024.
- Murphy, P., Summerhurst, K., Brady, G., Vendrell, V., Frankel, P., Redmond, M., Maddock, J., Lillion-Connolly, S., Armit, C., Hill, B., et al.** (2021b). Wnt Pathway Analysis mapped gene-expression data. *Edinburgh DataShare*, 2022.2011.2001.
- Noelanders, R. and Vleminckx, K.** (2017). How Wnt Signaling Builds the Brain: Bridging Development and Disease. *Neuroscientist* **23**, 314-329.
- Ohno S** (1970). *Evolution by Gene Duplication* Springer Verlag, New York
- Osmundsen, A. M., Keisler, J. L., Taketo, M. M. and Davis, S. W.** (2017). Canonical WNT Signaling Regulates the Pituitary Organizer and Pituitary Gland Formation. *Endocrinology* **158**, 3339-3353.
- Piper, J. and Rutovitz, D.** (1985). Data structures for image processing in a C language and Unix environment. *Pattern Recognit. Lett.* **3**, 119-129.
- Ryan, J. F., Pang, K., Schnitzler, C. E., Nguyen, A. D., Moreland, R. T., Simmons, D. K., Koch, B. J., Francis, W. R., Havlak, P., Smith, S. A., et al.** (2013). The genome of the ctenophore *Mnemiopsis leidyi* and its implications for cell type evolution. *Science* **342**, 1242592.
- Shannon, P., Markiel, A., Ozier, O., Baliga, N. S., Wang, J. T., Ramage, D., Amin, N., Schwikowski, B. and Ideker, T.** (2003). Cytoscape: a software environment for integrated models of biomolecular interaction networks. *Genome Res* **13**, 2498-2504.
- Singh, P. N. P., Shea, C. A., Sonker, S. K., Rolfe, R. A., Ray, A., Kumar, S., Gupta, P., Murphy, P. and Bandyopadhyay, A.** (2018). Precise spatial restriction of BMP signaling in developing joints is perturbed upon loss of embryo movement. *Development* **145**.
- Somorjai, I. M. L., Martí-Solans, J., Diaz-Gracia, M., Nishida, H., Imai, K. S., Escrivà, H., Cañestro, C. and Albalat, R.** (2018). Wnt evolution and function shuffling in liberal and conservative chordate genomes. *Genome Biol* **19**, 98.
- Summerhurst, K., Stark, M., Sharpe, J., Davidson, D. and Murphy, P.** (2008). 3D representation of Wnt and Frizzled gene expression patterns in the mouse embryo at embryonic day 11.5 (Ts19). *Gene Expr Patterns* **8**, 331-348.
- Theiler, K.** (1989). *The house mouse: Atlas of embryonic development*. New York: Springer Verlag.
- Tian, A., Benchabane, H. and Ahmed, Y.** (2018). Wingless/Wnt Signaling in Intestinal Development, Homeostasis, Regeneration and Tumorigenesis: A *Drosophila* Perspective. *J Dev Biol* **6**.
- Vacik, T., Stubbs, J. L. and Lemke, G.** (2011). A novel mechanism for the transcriptional regulation of Wnt signaling in development. *Genes Dev* **25**, 1783-1795.
- Vendrell, V., Summerhurst, K., Sharpe, J., Davidson, D. and Murphy, P.** (2009). Gene expression analysis of canonical Wnt pathway transcriptional regulators during early morphogenesis of the facial region in the mouse embryo. *Gene Expr Patterns* **9**, 296-305.

- Wang, Y., Zhou, C. J. and Liu, Y.** (2018). Wnt Signaling in Kidney Development and Disease. *Prog Mol Biol Transl Sci* **153**, 181-207.
- Yushkevich, P. A., Piven, J., Hazlett, H. C., Smith, R. G., Ho, S., Gee, J. C. and Gerig, G.** (2006). User-guided 3D active contour segmentation of anatomical structures: significantly improved efficiency and reliability. *Neuroimage* **31**, 1116-1128.
- Zhao, L., Saito, H., Sun, X., Shiota, K. and Ishibashi, M.** (2010). Sonic hedgehog is involved in formation of the ventral optic cup by limiting Bmp4 expression to the dorsal domain. *Mech Dev* **127**, 62-72.

Figures and Table

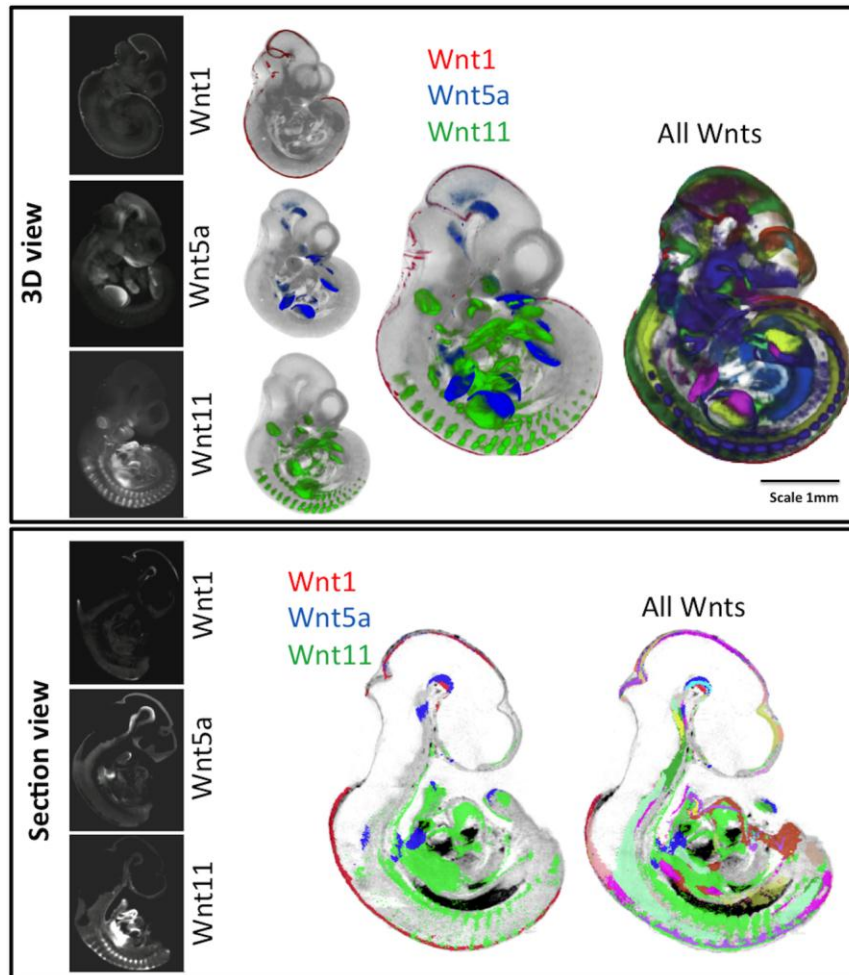


Fig. 1: Visualisation of mapped and integrated gene expression patterns, exemplified at E10.5. Upper panel; whole embryo external views of 3D data. The original OPT reconstructions showing the expression of Wnt1, Wnt5a and Wnt11 are on the left and individually mapped to the same reference model in the next column (see full 3D movies of each in Supplementary data movies S1-3). The right-hand columns show the three patterns integrated and all Wnt expression patterns integrated (see 3D movies S4, S5). The lower panel shows virtual sagittal section views through the same 3D data, showing original OPT data and mapped data as above. Red; Wnt1, green; Wnt11, blue; Wnt5a. For more detail on visualization of each pattern see Movie S5.

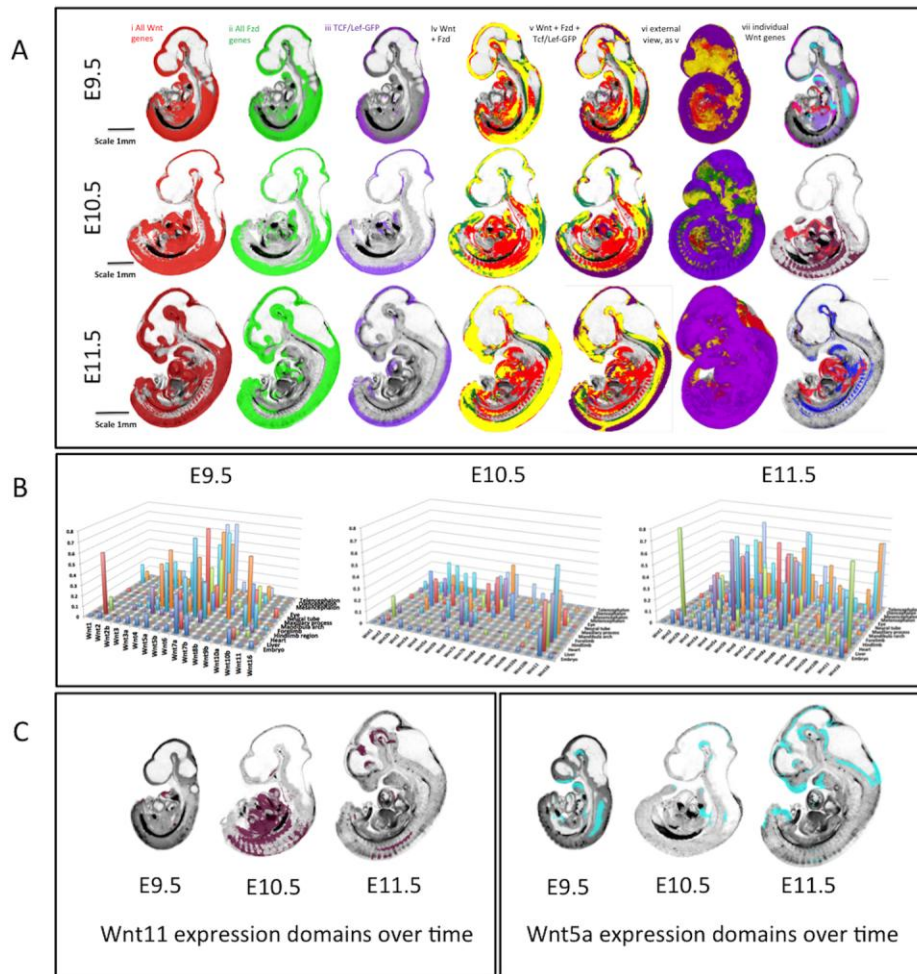


Fig. 2. Overview of integrated expression patterns. 2A shows union of the expression of all Wnt genes (red i) all Fzd genes (green ii) and the canonical pathway readout reporter (purple iii) across the three stages of development as indicated. Column iv shows the “all-Fzd” domain overlaid on the “all-Wnt” domain with overlap shown in yellow. Columns v and vi add the canonical read-out domain in purple (vi is an external view). Column vii shows individual Wnt expression patterns that contribute to the ventral Wnt domain (red; Wnt2, purple; Wnt10b, pink; Wnt4, pale blue; Wnt5a, dark red; Wnt11, dark blue; Wnt5b). 2B presents 3D graphs showing the extent (proportional size) of each Wnt gene domain in the whole embryo and in individual anatomical domains across stages as indicated; the y-axis shows the proportion of the anatomical domain (z axis) occupied by each gene expression domain (x axis). 2C shows Wnt11 and Wnt5a expression domains on midline sagittal sections across stages; these patterns illustrate the dynamic changes in extent of expression across stages

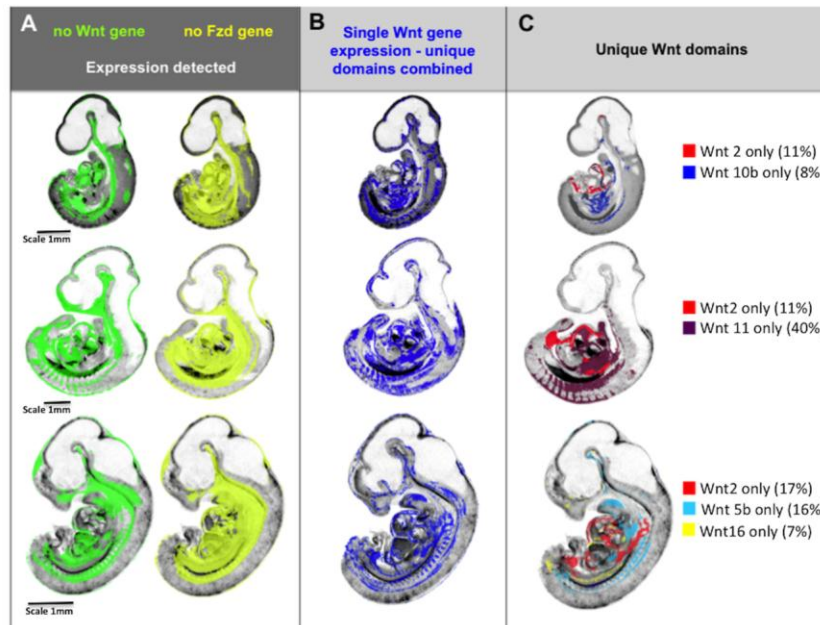


Fig. 3: Integrative mapping of all Wnt and Fzd domains allows visualization of the territories where no Wnt or Fzd gene is expressed (A) or where unique Wnt genes are expressed (B and C). A) domains across stages where no Wnt expression (green) or no Fzd expression (yellow) is detected. **B)** domains across stages where a single Wnt gene is detected i.e. unique detection of a single Wnt gene transcript. **C)** individual Wnt gene domains that account for much of the single Wnt gene domain at each stage i.e. much of the unique Wnt gene territory in the ventral embryo at E10.5 is occupied by Wnt2 and Wnt11 expression domains whereas Wnt11 contributes little at E11.5 when Wnt5b is more prominent. The figures noted in brackets are the percentage of the unique Wnt gene expression domain at that stage contributed to by that gene. Note that the unique Wnt domains reported here were obtained by subtraction of multiple mapped expression domains and, as such, are sensitive to cumulate effects of noise in the data for each gene, in particular small differences in thresholding the original, continuously variable signals into binary (expressed versus not detected) values. While the images show the general location of the domains, the boundaries should be considered as approximate.

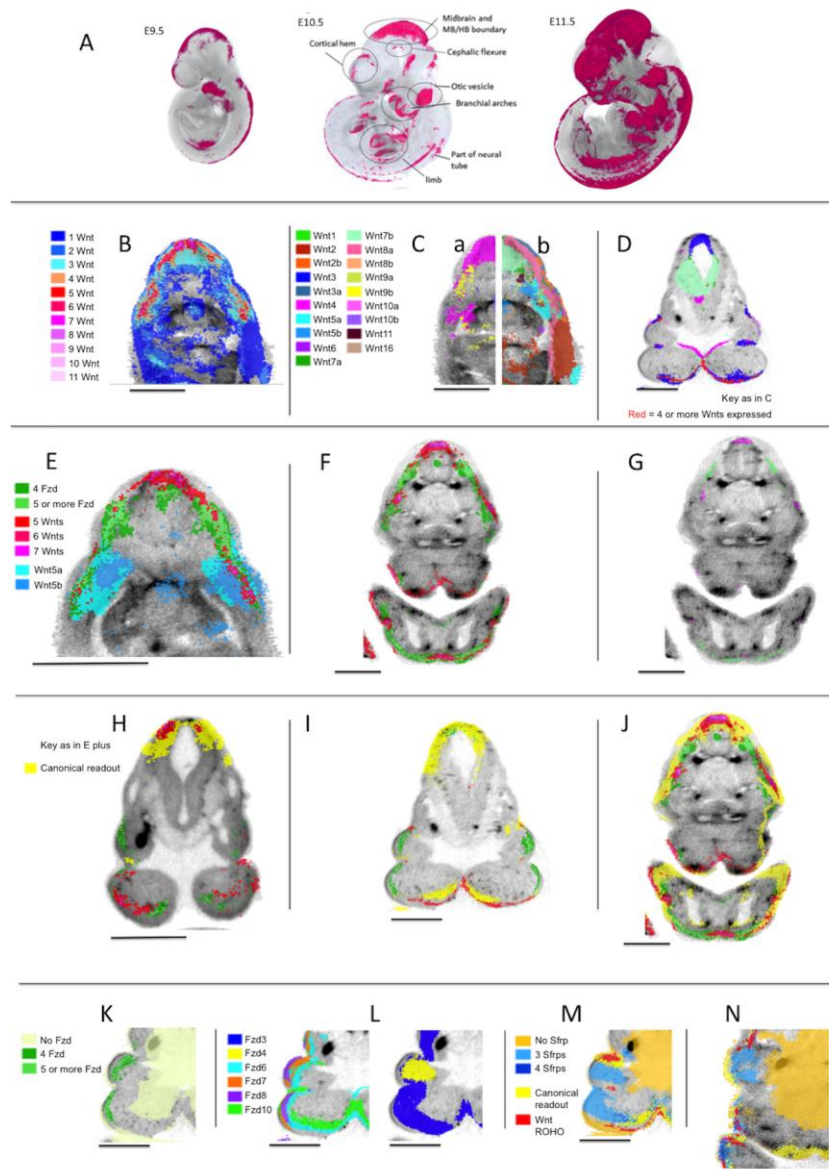


Fig. 4: Regions of high occupancy Wnt and Fzd expression.

A) Regions of high occupancy of Wnt gene expression (red) at E9.5, E10.5 and E11.5.

B) Transverse section through an OPT reference model of an E11.5 embryo in the mid-flank region showing the distribution of occupancy of Wnt expression as indicated. This section reveals three Regions of High Occupancy (ROHOs)

C) Same section as B, showing the mapped expression of individual Wnt genes as indicated. For clarity, (a) left and (b) right halves of the section are shown with the expression of (a) Wnts 3, 4, 8b, 9b, 10a, 10b and (b) Wnts 1, 2, 2b, 3a, 5a, 5b, 6, 7a, 7b, 8a, 9a, 11, 16.

D) A section through an OPT reference model of an E10.5 embryo in the mandibular region. Regions of high occupancy of Wnt expression (Red; 4 or more Wnts expressed) and individual Wnt gene expression domains are shown for Wnts 3, 4, 7a, 7b, 10a and 10b (key as in C).

E) Transverse section through an OPT reference model of an E11.5 embryo in the mid-flank region showing Fzd ROHOs (key as indicated) in the context of Wnt ROHOs (key as in B showing only 5+ Wnt genes) and expression of Wnt5a and Wnt5b.

F) Transverse section through an OPT reference model of an E11.5 embryo in the mandibular region showing Wnt and Fzd ROHOs (key as in E).

G) The same section as in F, showing only the peaks of Wnt and Fzd occupancy (Wnt occupancy of 7 and more; Fzd occupancy of 6 and more).

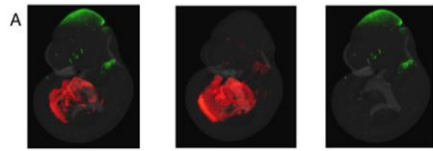
H, I, J) sections through the mandibular region in OPT reference models of embryos at E9.5, 10.5 and 11.5 respectively. The images show the canonical pathway readout (Tcf/Lef-GFP RNA) (yellow) in the context of Wnt and Fzd ROHOs (key as in E).

K) Section through the mandibular region of an OPT reference model of an E10.5 embryo showing Fzd ROHOs compared with where no Fzds are detected (as indicated)

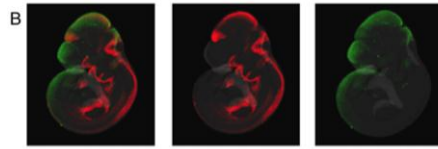
L) The same section as in K showing the expression of individual Fzds genes as indicated (the section is repeated for clarity).

M) The same section as in K showing Sfrp occupancy 0, 3 and 4 (as indicated) in the context of Wnt ROHOs (key as in E) and canonical pathway readout (Tcf/Lef-GFP) in yellow.

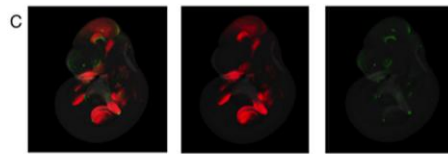
N) The same key as M on a section through the maxillary and mandibular region of an OPT reference model of an E11.5 embryo.



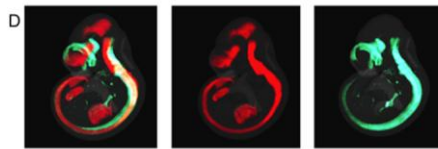
Wnt2b
0.004
Wnt2
0.003
0.07
0.06
Wnt2 and Wnt2b



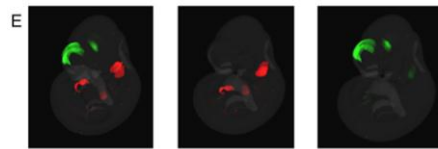
Wnt3a
0.03
Wnt3
0.11
0.07
0.29
Wnt3 and Wnt3a



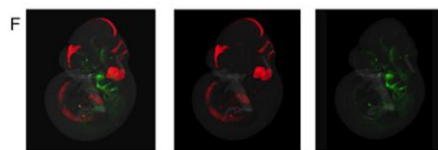
Wnt5b
0.0012
Wnt5a
0.014
0.03
0.34
Wnt5a and Wnt5b



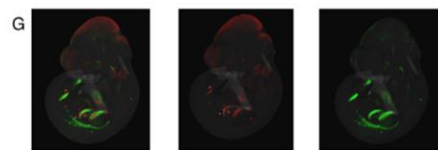
Wnt7b
0.08
Wnt7a
0.45
0.06
0.34
Wnt7a and Wnt7b



Wnt8b
0.008
Wnt8a
0.003
0.01
0.003
Wnt8a and Wnt8b



Wnt9b
0.006
Wnt9a
0.006
0.02
0.02
Wnt9a and Wnt9b



Wnt10b
0.004
Wnt10a
0.02
0.03
0.16
Wnt10a and Wnt10b

Fig. 5: Comparison of expression of paralogous pairs of Wnt genes at E10.5 mapped to the reference embryo model. Each row shows a different pair of the seven Wnt paralogues, as indicated. The combined image of both genes is shown on the left and the two individual patterns in the order listed from left to right (colour coded). The rubric indicates the relative size of each domain (e.g. Wnt2 occupies 7% of the embryo); the intersecting numbers show the proportion of one pattern overlapping the other so 6% of the Wnt2b domain overlaps the Wnt2 domain. Note the highest level of overlap for the Wnt7 paralogues, followed by the Wnt3 and Wnt5 paralogues.

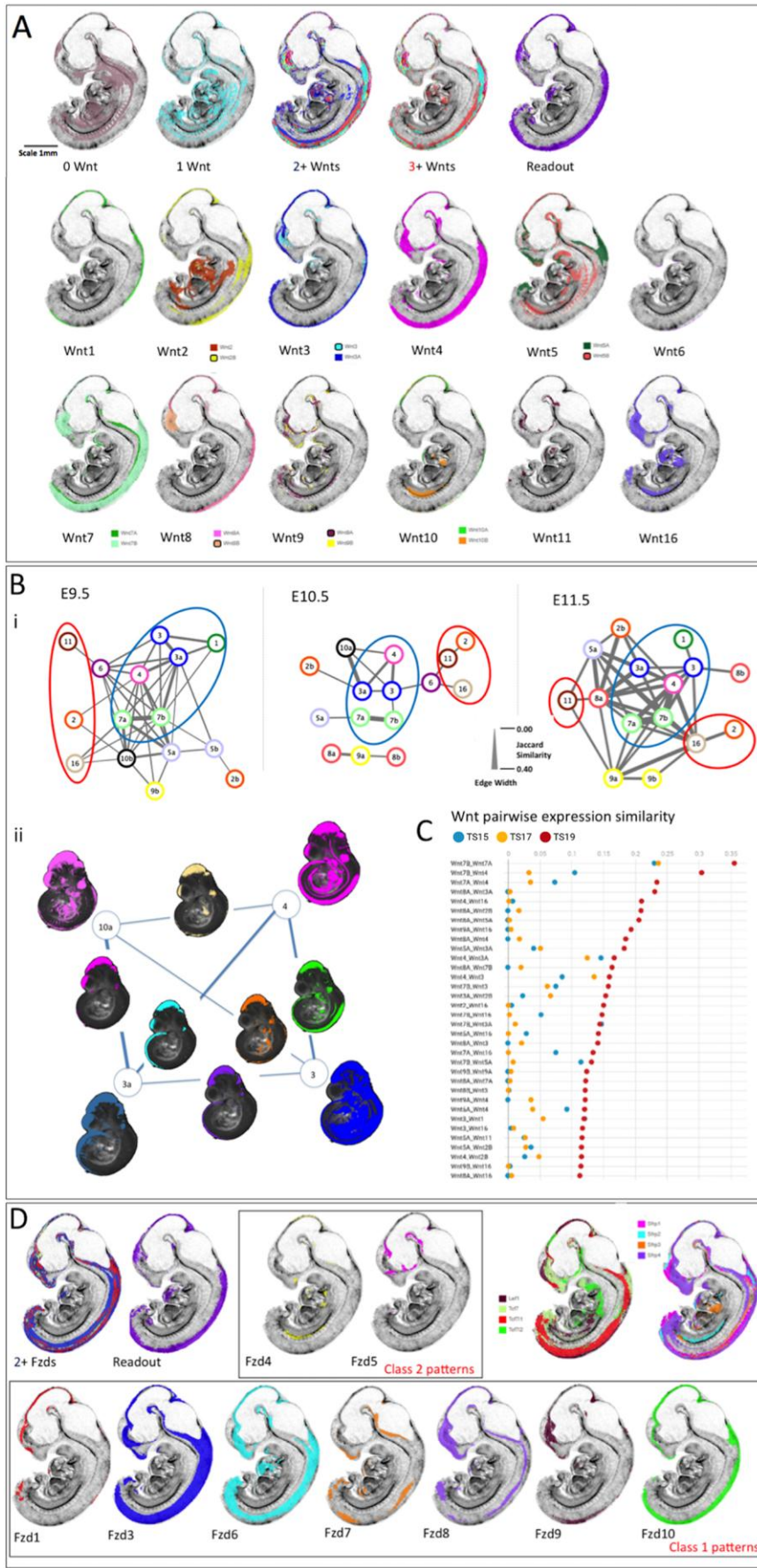


Fig. 6: Integrated comparison of gene expression pattern similarity across Wnt, Fzd and other pathway component genes.

A) E11.5 example of the visual analysis carried out; all virtual sections are identical, mid-sagittal. The top row shows the territories where zero Wnts are detected (0 Wnt), where individual Wnt genes are expressed uniquely (1 Wnt), where 2 or more (2+ Wnts) or 3 or more (3+ Wnts) genes are co-expressed and where canonical Wnt pathway readout is detected (Tcf/Lef-GFP). Rows 2 and 3 represent mapped expression of each of the Wnt family genes as indicated. The analysis included viewing the full set of sections in all orientations and across stages.

Bi) Network diagrams representing the similarities between Wnt expression pattern across time. The lines connecting nodes represent the Jaccard Index (JI) of similarity (intersection/union), with thickness scaled as shown. Each “node” represents a Wnt gene as indicated (e.g. 3a=Wnt3a). For comparison of the network, thresholds were adjusted to show the 15 genes with expression patterns most similar to other Wnt genes at each stage. Blue circles enclose the group with most highly similar expression patterns, consistent across stages (Group 1). Red circles enclose the most divergent expression patterns (Group 3).

Bii) illustrates visually the nature of the lines connecting genes in the network focussing on the most highly connected genes at E10.5; Wnts 3, 3a, 4 and 10a. The mapped Wnt expression patterns are shown here in projection through a 3D view of the reference model embryo, at each corner of the network (as indicated). Intersection domains, where each pair of expression patterns intersect, are shown on the lines connecting that gene pair.

C) Top 34 similarity scores among all Wnt genes across stages. The horizontal axis refers to Jaccard Index. (red, E11.5; blue E10.5; yellow, E9.5).

D) Domains of multiple Fzd expression patterns (2+ Fzds) correspond well to territories of canonical pathway readout (Tcf-Lef-GFP). Fzd expression patterns fall within two classes: class 1 (row 2) are similar to canonical readout, Tcf/Lef transcription factor and Sfrp family member expression patterns (row 1, right). Example patterns at E11.5 are shown.

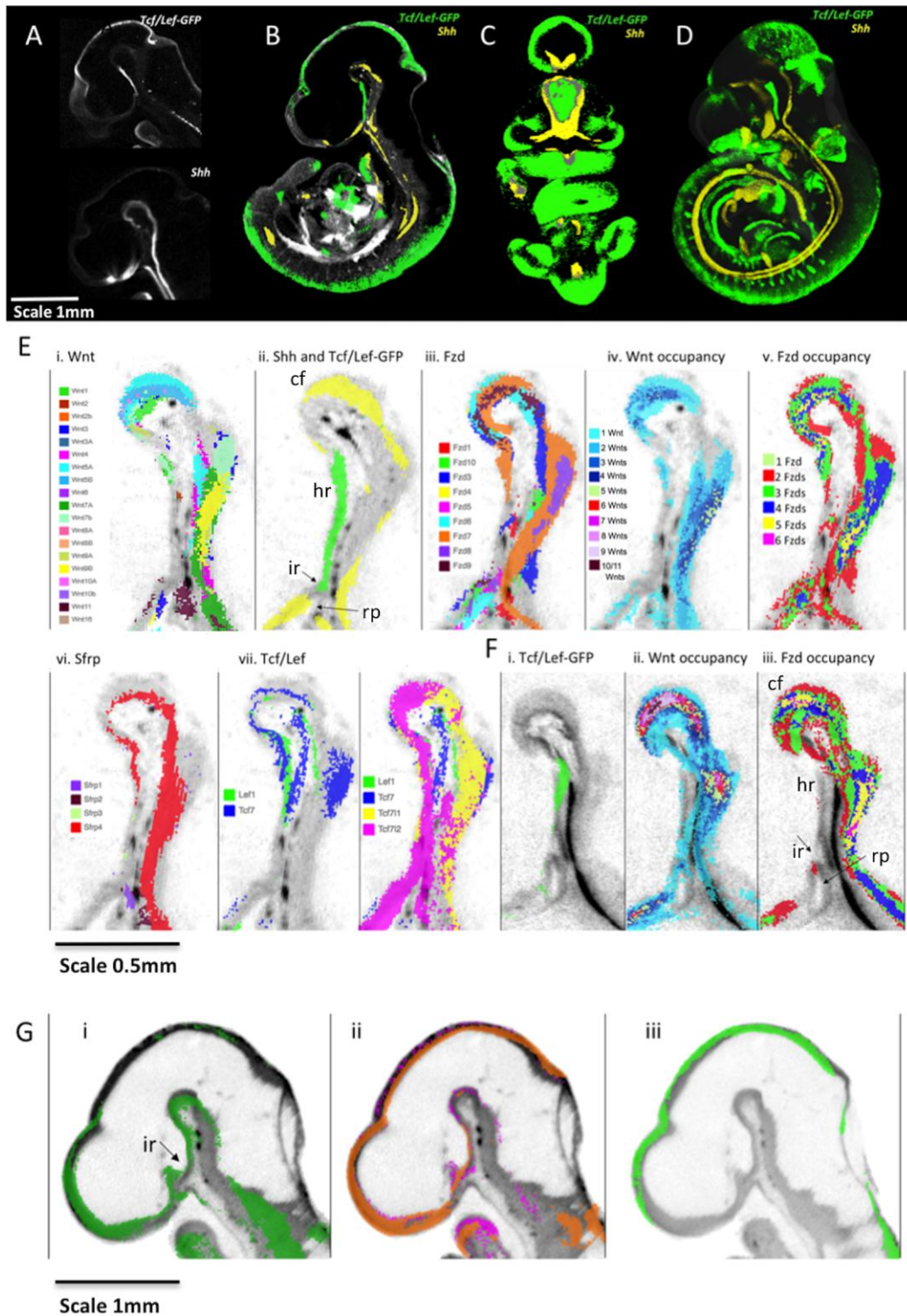


Fig. 7: Integrated expression patterns in the Ventral Diencephalon: Complementary expression of *Shh* and canonical Wnt pathway readout.

A) *Tcf/Lef-GFP* readout pattern and *Shh* expression in virtual sagittal sections through the diencephalon of raw OPT data. B-D) Mapped data with grayscale render of the 3D model showing anatomy. B shows a virtual sagittal section through the 3D model emphasising the complementary

expression of Tcf/Lef-GFP readout pattern (green) and Shh (yellow) in the ventral diencephalon. C is a thick virtual coronal section (288 μm) through the 3D model of mapped data again showing complementarity in the patterns (absence of overlap verified on serial sections) D is a full 3D representation (point cloud render). A-D, E10.5. Scale bar in C and D as for B.

E) Sagittal sections through the ventral diencephalon at E10.5 showing: i) mapped expression of all Wnt genes as indicated by the key; ii) canonical Wnt readout (Tcf/Lef-GFP, green) and Shh (yellow) expression on the same section; iii) mapped expression of all Fzd genes as indicated by the key; iv) Wnt occupancy; the number of Wnt genes co-expressed as indicated (no colour indicates zero Wnts are detected); v) Fzd occupancy; the number of Fzd genes co-expressed as indicated (no colour indicates zero genes detected); vi) mapped expression of Sfrp genes as indicated by key; vii) mapped expression of Tcf/Lef transcription factor genes as indicated by key.

F) Sagittal sections through the ventral diencephalon at E11.5 showing i) canonical Wnt readout (Tcf/Lef-GFP, green); ii) the number of Wnt genes co-expressed (key as in E iv) and iii) the number of Fzd genes co-expressed (key as in E v) (no colour indicates zero genes detected).

G) Sagittal sections through the brain at E9.5 showing i) mapped expression of Wnt7a (green), ii) mapped expression of Fzd5 (magenta) and Fzd7 (orange) and iii) canonical Wnt readout (Tcf/Lef-GFP, green). Abbreviations: *ir* infundibular recess; *rp* Rathke's pouch; *cf* cephalic flexure; *hp* future hypothalamus.

Table 1: Similarity indices (Jaccard (JI)) of expression domains of Wnt paralogous gene pairs over time (highest values are highlighted in grey)

	E9.5	E10.5	E11.5
Wnt2/ Wnt2b	0.003	0.003	0.05
Wnt3/ Wnt3a	0.164	0.083	0.11
Wnt5a/ Wnt5b	0.06	0.014	0.09
Wnt7a/ Wnt7b	0.23	0.24	0.36
Wnt8a/ Wnt8b	-	0.001	0.05
Wnt9a/ Wnt9b	-	0.004	0.12
Wnt10a/ Wnt10b	0.009	0.018	0.06

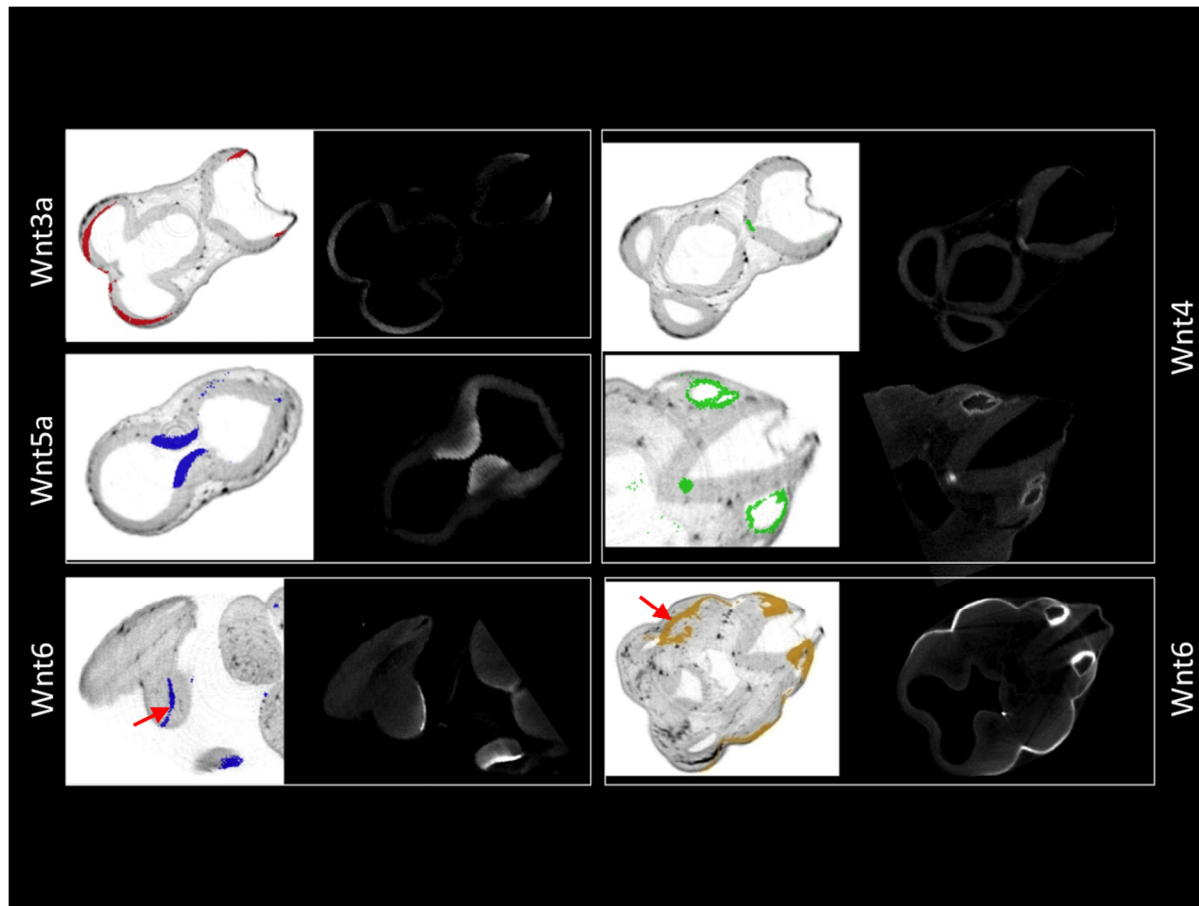


Fig. S1. Illustration of mapping accuracy using WlzWarp. Examples of mapped data (bright-field image on left) compared to equivalent virtual sections through 3D reconstructions of the original gene expression data (on right) for genes as indicated. All data are from E10.5 embryos through the forebrain and midbrain (Wnt3a, Wnt5a, Wnt4 (upper)), the hindbrain (Wnt4 lower), the forelimb (Wnt6 left) and hindbrain and forebrain (Wnt6 right). Note the mapping accuracy overall but the mis-mapping of ectodermal Wnt6 on one side of the embryo (arrows). Please note that mapped data are used for integrated analysis and any interpretation is supported by viewing the original scanned expression pattern. Relative scale as indicated on Figure 1.

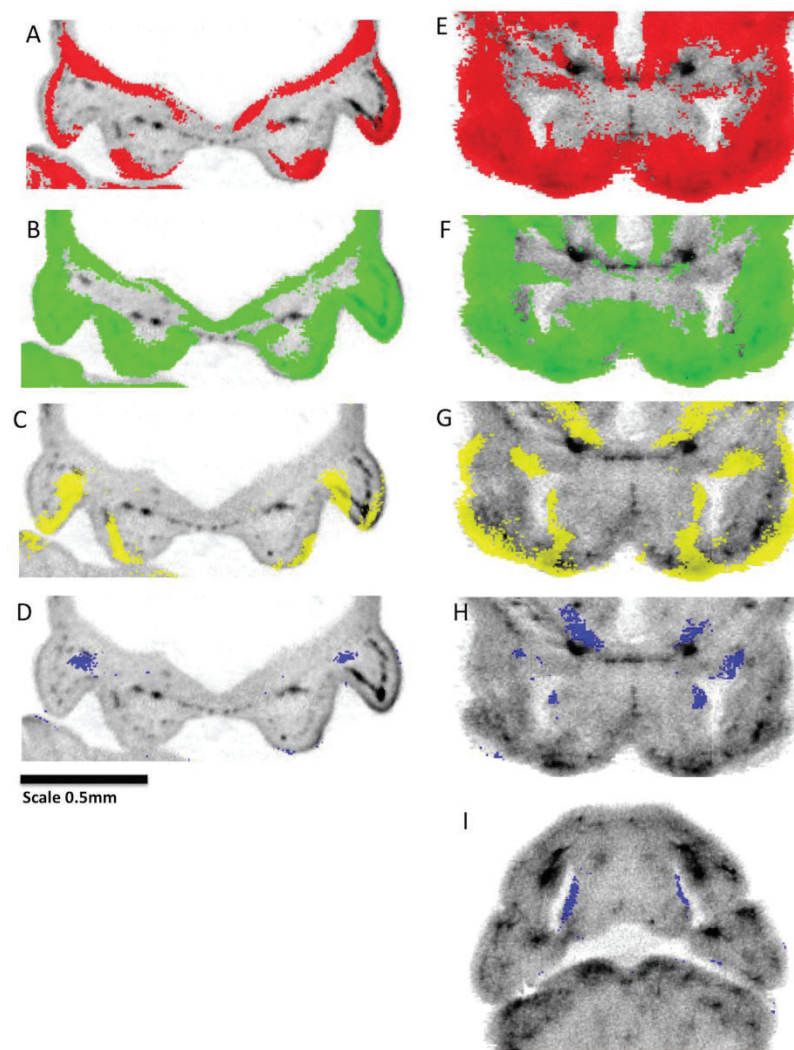


Fig S2. Canonical Wnt pathway activity in the context of detectable Wnt and Fzd expression in the nasal region. A-H: Frontal sections in the nasal region in OPT reference models of E10.5 (A-D) and E11.5 (E-H) embryos; I is a transverse section at E11.5. A and E, show combined expression domain for all Wnt genes; B and F, combined expression domain for all Fzd genes; C and G, Tcf/Lef-GFP; D, H and I shows the domain of Tcf/Lef-GFP activity where neither Wnt nor Fzd expression was detected.

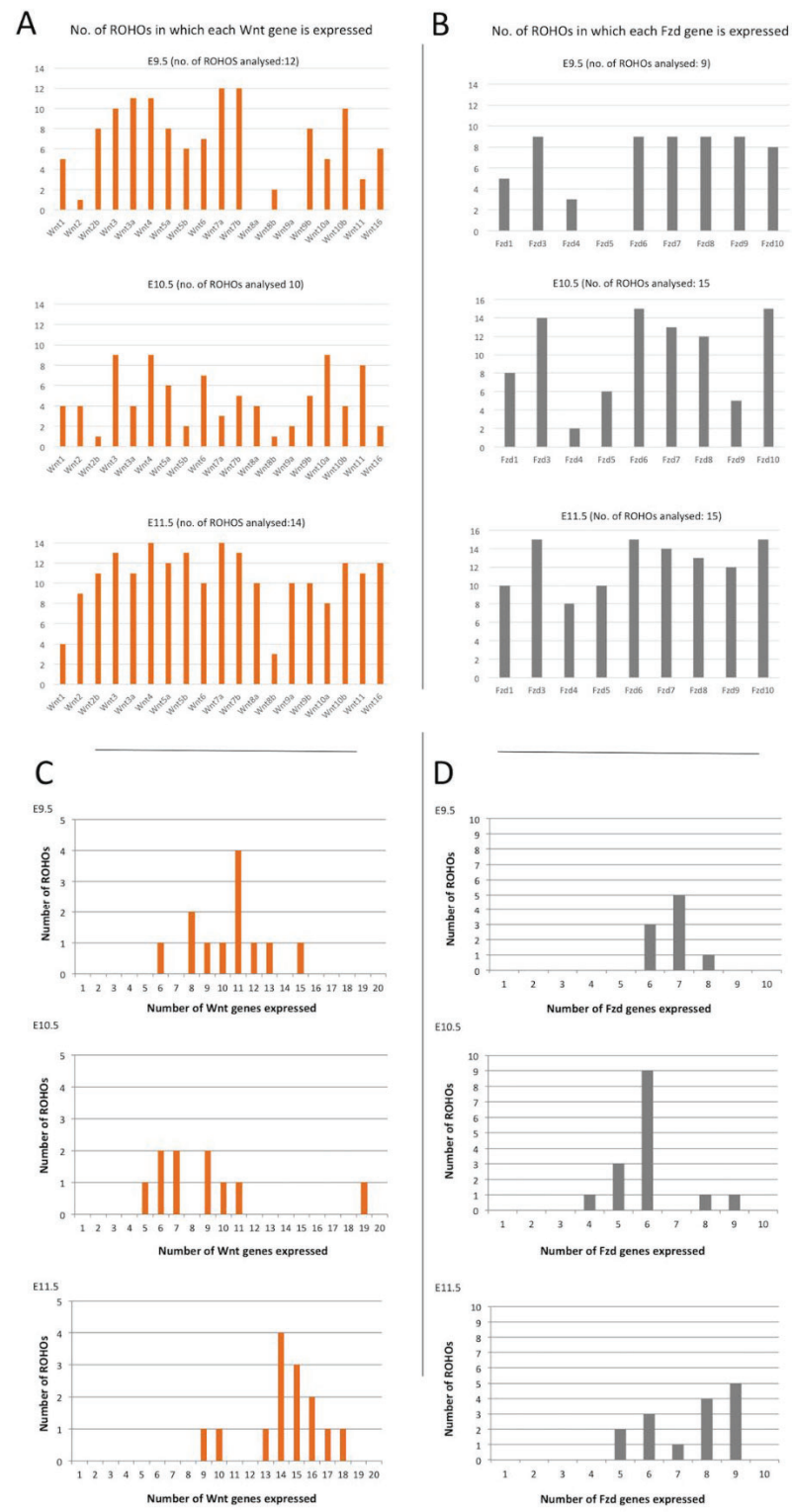


Fig. S3. Analysis of Wnt and Fzd ROHOs. A and B show the number of ROHOs in which each Wnt (A) and Fzd (B) gene are expressed, across stages. C and D graphically represent the number of Wnt (C) and Fzd (D) genes expressed per ROHO. Note the shift to more genes expressed per ROHO at E11.5

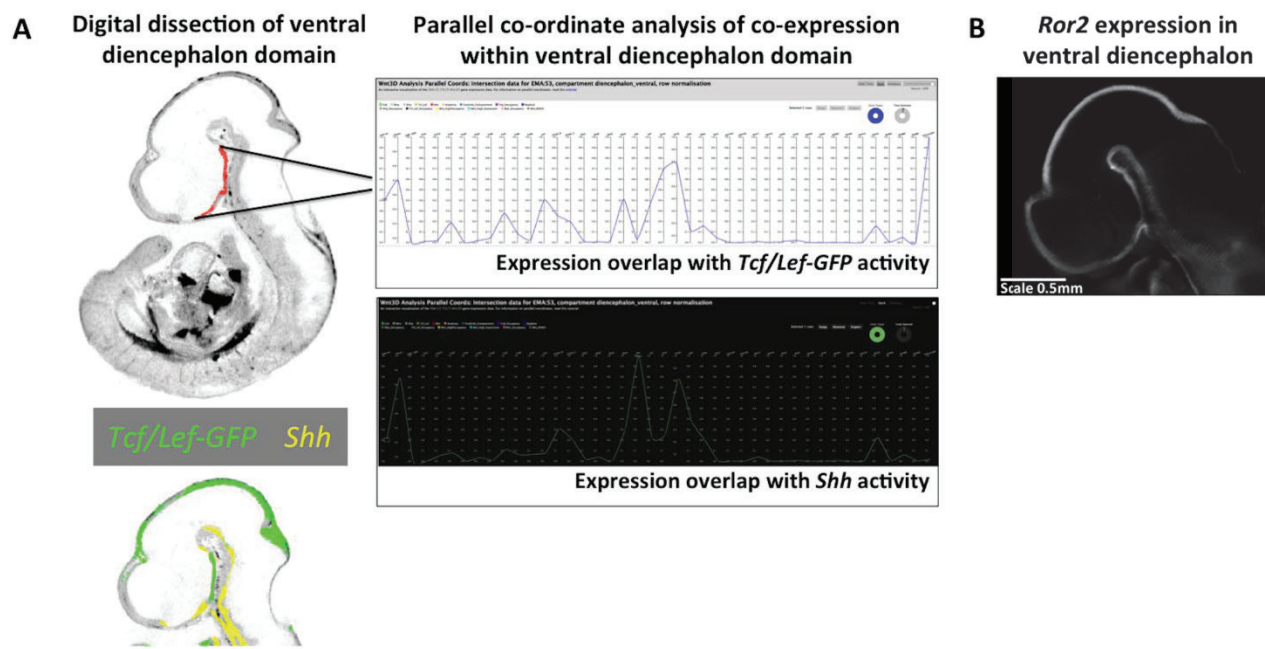


Fig. S4. Analysis of genes expressed in the ventral diencephalon. A represents the digital analysis of the full set of genes expressed using parallel co-ordinates of mapped data. B shows *Ror2* expression in an OPT reconstruction.

Table S1. Proportional Wnt Expression Volumes

Gene	Embryo			Liver			Heart			Hindlimb Region			Forelimb			Mandibular Arch			Maxillary Process			Neural Tube			Eye			Metencephalon			Mesencephalon			Diencephalon			Telencephalon		
	E9.5	E10.5	E11.5	E9.5	E10.5	E11.5	E9.5	E10.5	E11.5	E9.5	E10.5	E11.5	E9.5	E10.5	E11.5	E9.5	E10.5	E11.5	E9.5	E10.5	E11.5	E9.5	E10.5	E11.5	E9.5	E10.5	E11.5	E9.5	E10.5	E11.5	E9.5	E10.5	E11.5	E9.5	E10.5	E11.5			
Wnt1	0.0183	0.0108	0.0171	0.0000	0.0001	0.0004	0.0005	0.0003	0.0035	0.0000	0.0000	0.0006	0.0000	0.0000	0.0000	0.0001	0.0000	0.0000	0.0001	0.0001	0.0000	0.030	0.034	0.034	0.000	0.001	0.000	0.000	0.035	0.054	0.193	0.073	0.129	0.088	0.015	0.016	0.008	0.000	0.003
Wnt2	0.0498	0.0681	0.1134	0.5845	0.0389	0.0904	0.1287	0.1819	0.7694	0.0073	0.0625	0.0074	0.003	0.001	0.029	0.009	0.000	0.024	0.000	0.004	0.009	0.000	0.000	0.000	0.000	0.010	0.096	0.000	0.002	0.015	0.000	0.000	0.000	0.000	0.000	0.000	0.001	0.001	0.001
Wnt2b	0.0115	0.0035	0.1230	0.0001	0.0000	0.0000	0.0014	0.0001	0.0329	0.0091	0.0003	0.0186	0.006	0.000	0.093	0.005	0.000	0.061	0.006	0.005	0.101	0.007	0.000	0.259	0.007	0.017	0.206	0.000	0.002	0.046	0.021	0.088	0.199	0.016	0.007	0.005	0.005	0.000	0.016
Wnt3	0.0327	0.0714	0.0550	0.0018	0.0050	0.0002	0.0019	0.0214	0.0519	0.0525	0.0176	0.0147	0.041	0.054	0.028	0.010	0.112	0.035	0.043	0.317	0.038	0.038	0.218	0.075	0.009	0.040	0.003	0.000	0.168	0.131	0.252	0.293	0.337	0.042	0.138	0.254	0.001	0.001	0.206
Wnt3a	0.0705	0.0262	0.1417	0.0000	0.0000	0.0014	0.0001	0.0003	0.0009	0.0182	0.0090	0.3740	0.063	0.000	0.319	0.097	0.000	0.029	0.031	0.000	0.131	0.123	0.049	0.123	0.017	0.008	0.100	0.000	0.026	0.061	0.275	0.272	0.465	0.152	0.093	0.119	0.119	0.143	0.272
Wnt4	0.0849	0.0411	0.1567	0.0004	0.0067	0.0005	0.0140	0.0342	0.1991	0.2570	0.0024	0.0158	0.103	0.003	0.041	0.414	0.018	0.034	0.209	0.012	0.084	0.118	0.184	0.451	0.015	0.004	0.013	0.000	0.024	0.080	0.082	0.214	0.527	0.078	0.035	0.486	0.060	0.018	0.649
Wnt5a	0.1255	0.0298	0.1981	0.0035	0.0000	0.0002	0.0100	0.0027	0.0401	0.0587	0.0845	0.6995	0.391	0.157	0.704	0.563	0.011	0.193	0.003	0.000	0.522	0.112	0.005	0.057	0.003	0.000	0.025	0.000	0.020	0.253	0.297	0.234	0.327	0.139	0.036	0.197	0.012	0.000	0.169
Wnt5b	0.0228	0.0012	0.1110	0.0003	0.0000	0.0614	0.0039	0.0004	0.1450	0.0399	0.0011	0.0706	0.009	0.000	0.076	0.002	0.000	0.204	0.000	0.078	0.123	0.005	0.000	0.076	0.012	0.011	0.342	0.000	0.001	0.045	0.144	0.012	0.335	0.062	0.006	0.135	0.090	0.002	0.093
Wnt6	0.0619	0.0858	0.0262	0.0012	0.0000	0.0001	0.0037	0.0230	0.0064	0.1767	0.2243	0.1157	0.362	0.172	0.103	0.149	0.224	0.042	0.094	0.003	0.134	0.014	0.032	0.002	0.002	0.114	0.029	0.000	0.085	0.002	0.104	0.057	0.001	0.031	0.006	0.000	0.000	0.007	0.003
Wnt7a	0.3555	0.0614	0.1494	0.1613	0.0000	0.0063	0.0175	0.0002	0.0484	0.0223	0.1318	0.0268	0.736	0.097	0.047	0.533	0.000	0.036	0.272	0.006	0.020	0.748	0.252	0.615	0.343	0.000	0.005	0.000	0.198	0.439	0.517	0.238	0.441	0.620	0.131	0.385	0.673	0.222	0.312
Wnt7b	0.1863	0.0814	0.1547	0.0037	0.0024	0.0009	0.0099	0.0014	0.0059	0.1159	0.0000	0.0444	0.340	0.003	0.059	0.116	0.018	0.101	0.177	0.073	0.115	0.217	0.318	0.527	0.439	0.095	0.139	0.000	0.256	0.414	0.648	0.000	0.354	0.508	0.327	0.483	0.686	0.212	0.604
Wnt8a	0.0000	0.0099	0.1340	0.0000	0.0033	0.0104	0.0000	0.0400	0.0076	0.0000	0.0000	0.2404	0.000	0.000	0.373	0.000	0.004	0.068	0.000	0.002	0.168	0.000	0.001	0.151	0.000	0.001	0.140	0.000	0.010	0.141	0.000	0.001	0.642	0.000	0.001	0.249	0.000	0.000	0.155
Wnt8b	0.0054	0.0075	0.0199	0.0005	0.0000	0.0004	0.0013	0.0000	0.0011	0.0050	0.0000	0.0001	0.000	0.000	0.000	0.001	0.000	0.000	0.000	0.237	0.000	0.000	0.000	0.000	0.000	0.000	0.000	0.000	0.000	0.000	0.000	0.000	0.000	0.000	0.000	0.000	0.000	0.000	0.000
Wnt9a	0.0000	0.0188	0.0915	0.0000	0.0050	0.0042	0.0000	0.0447	0.1288	0.0000	0.0000	0.0062	0.000	0.000	0.001	0.000	0.000	0.003	0.000	0.000	0.008	0.000	0.001	0.017	0.000	0.000	0.030	0.000	0.007	0.126	0.000	0.048	0.227	0.000	0.014	0.359	0.000	0.073	0.222
Wnt9b	0.0241	0.0058	0.0595	0.0005	0.0019	0.0299	0.0068	0.0039	0.0172	0.0065	0.0002	0.0316	0.017	0.001	0.021	0.430	0.060	0.115	0.071	0.005	0.185	0.008	0.000	0.007	0.049	0.012	0.105	0.000	0.007	0.123	0.000	0.001	0.141	0.037	0.003	0.187	0.073	0.002	0.126
Wnt10a	0.0048	0.0287	0.0138	0.0002	0.0273	0.0001	0.0000	0.0133	0.0198	0.0001	0.0121	0.0006	0.001	0.023	0.004	0.000	0.007	0.000	0.000	0.000	0.001	0.006	0.007	0.009	0.032	0.038	0.000	0.000	0.033	0.003	0.002	0.304	0.188	0.026	0.085	0.006	0.015	0.082	0.097
Wnt10b	0.1359	0.0036	0.0236	0.1056	0.0001	0.0084	0.0416	0.0010	0.1765	0.0305	0.0269	0.0155	0.203	0.037	0.029	0.609	0.000	0.019	0.324	0.000	0.051	0.234	0.000	0.010	0.236	0.000	0.001	0.000	0.000	0.003	0.076	0.001	0.128	0.134	0.002	0.003	0.086	0.001	0.005
Wnt11	0.0177	0.2219	0.0580	0.0000	0.4035	0.0018	0.0550	0.3513	0.0953	0.0729	0.3941	0.1605	0.225	0.593	0.330	0.028	0.360	0.003	0.000	0.001	0.063	0.003	0.141	0.019	0.000	0.042	0.008	0.000	0.027	0.029	0.000	0.002	0.085	0.005	0.024	0.190	0.000	0.015	0.098
Wnt16	0.0603	0.0321	0.1576	0.0159	0.0000	0.0824	0.0161	0.0000	0.6911	0.0095	0.0002	0.0275	0.033	0.001	0.014	0.011	0.002	0.032	0.006	0.016	0.049	0.087	0.010	0.009	0.003	0.001	0.014	0.000	0.011	0.100	0.000	0.000	0.389	0.001	0.000	0.611	0.001	0.001	0.590

Table S2.

- (i) Proportion of the single-Wnt gene expression domain occupied by each Wnt across stages

Wnt gene	9.5 dpc	10.5 dpc	11.5 dpc
Wnt1	0.00684	0.00861	0.00454
Wnt2b	0.00466	0.00073	0.08383
Wnt2	0.07945	0.10506	0.16993
Wnt3a	0.02398	0.01722	0.07222
Wnt3	0.01189	0.06084	0.00597
Wnt4	0.0538	0.02939	0.03607
Wnt5a	0.07124	0.02666	0.11043
Wnt5b	0.00835	0.00074	0.16437
Wnt6	0.03493	0.09375	0.00921
Wnt7a	0.39379	0.05526	0.07819
Wnt7b	0.10618	0.09457	0.03283
Wnt8a	0	0.0059	0.02262
Wnt8b	0.00159	0.0053	0.003
Wnt9a	0	0.01962	0.06795
Wnt9b	0.01084	0.00259	0.02925
Wnt10a	0.00186	0.02698	0.00243
Wnt10b	0.1139	0.00136	0.01015
Wnt11	0.01592	0.39775	0.02279
Wnt16	0.06071	0.0476	0.07415

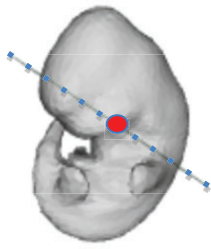
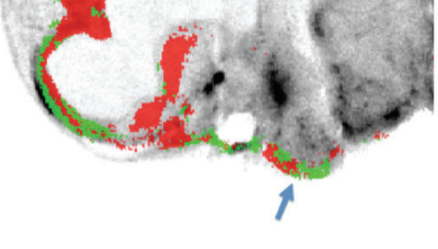
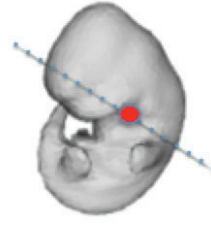
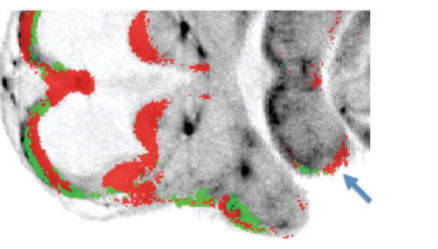
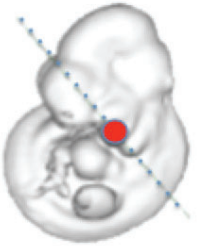
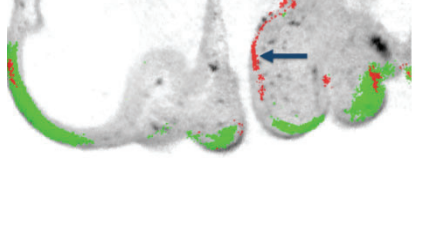
- (ii) Proportions of each Wnt gene expression domain (and canonical read-out) within the single Wnt expression domain (normalised by the individual Wnt expression domain volume).

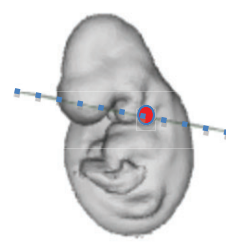
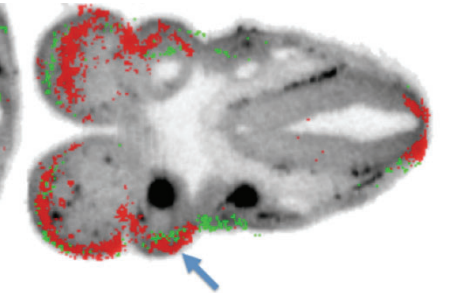
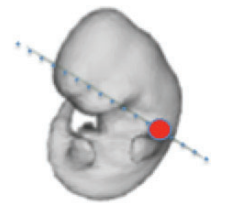
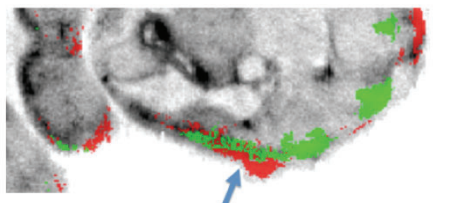
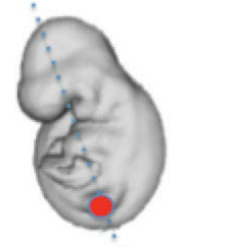
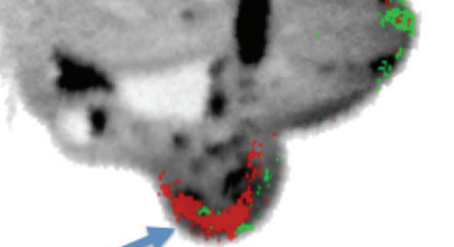
Wnt	9.5 dpc	10.5 dpc	11.5 dpc
Wnt1	0.11466	0.28179	0.06599
Wnt2	0.48927	0.54252	0.37266


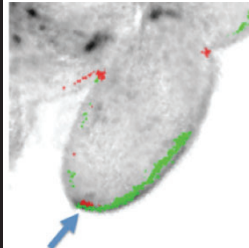
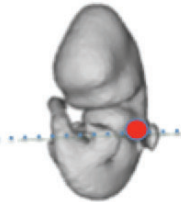
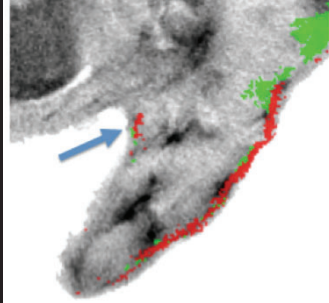
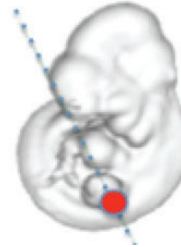
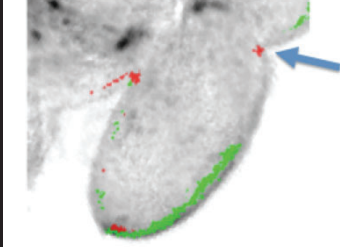
Wnt2b	0.1242	0.07291	0.16949
Wnt3	0.11151	0.29977	0.02701
Wnt3a	0.10426	0.23143	0.12668
Wnt4	0.1944	0.25136	0.05721
Wnt5a	0.17406	0.31449	0.13857
Wnt5b	0.11239	0.21475	0.36803
Wnt6	0.1731	0.3844	0.0875
Wnt7a	0.3396	0.31664	0.13011
Wnt7b	0.17472	0.40856	0.05277
Wnt8a	0	0.20901	0.04197
Wnt8b	0.09059	0.24741	0.03749
Wnt9a	0	0.3669	0.18468
Wnt9b	0.13795	0.15841	0.12216
Wnt10a	0.11904	0.3306	0.04382
Wnt10b	0.25689	0.13489	0.10676
Wnt11	0.27627	0.63064	0.09769
Wnt16	0.30858	0.52106	0.11702
Canonical readout	0.31377	0.35058	0.18978

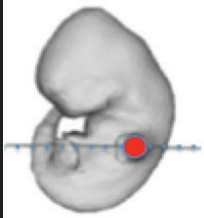
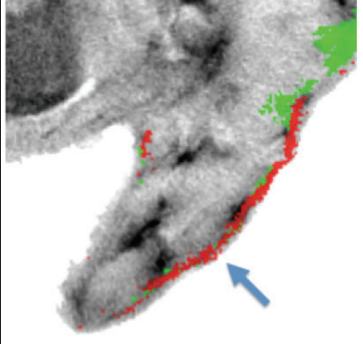
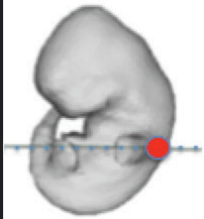
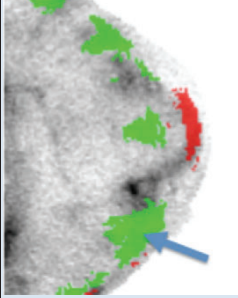
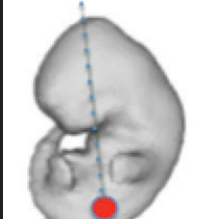
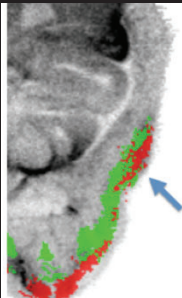
Note that the domains represented in Supplementary Table 2 were obtained by subtraction of multiple mapped expression domains and, as such, are sensitive to cumulative effects of noise in the data for each gene, in particular small differences in thresholding the original, continuously variable signals into binary (expressed versus not detected) values. The volumes should therefore be considered as approximate.

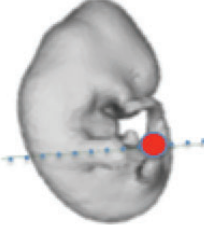
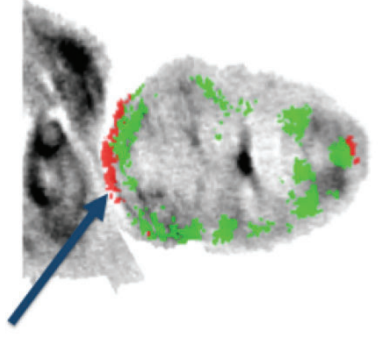
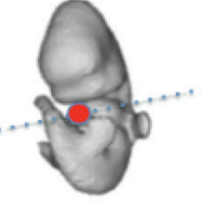
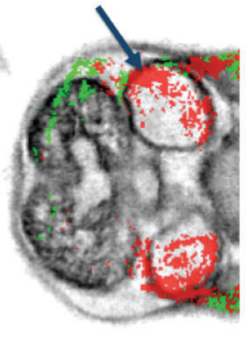
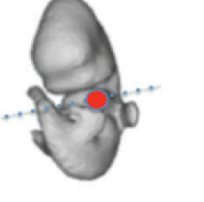
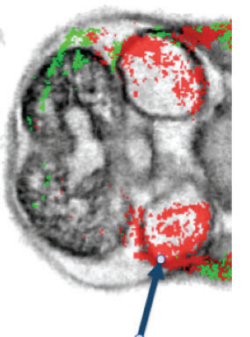
Table S3. Genes expressed in each of the Wnt and Fzd ROHOs examined. Right hand columns show location with Wnt ROHO in red and Fzd ROHO in green

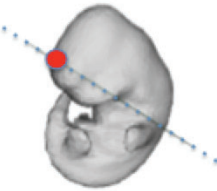
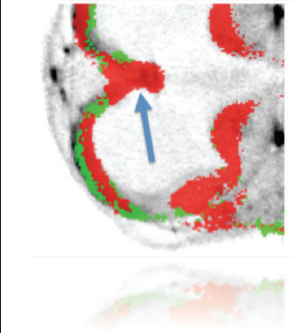
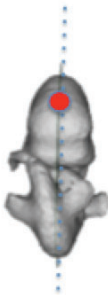
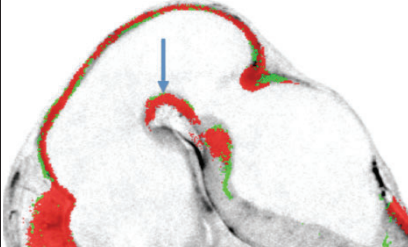
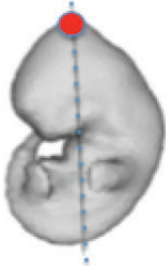
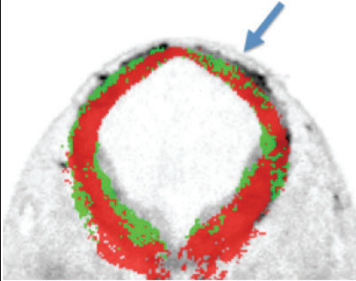
STRUCTURE	ROHO	E9.5 set	E10.5 set	E11.5set	Location	Wnt ROHO and Fzd ROHO
Maxilla	W1	2b, 3, 3a, 4, 6, 7a, 7b, 9b, 10b	2, 3, 3a, 4, 5a, 6, 7b, 9b, 10a, 11	2, 2b, 3, 3a, 4, 5a, 5b, 6, (7a), 7b, 8a, 9a, 9b, 10b, 11, (16)		
Maxilla	F1	1, 3, 4, 6, 7, 8, (9), (10)	(1), 3, 6, 7, 8, 10	1, 3, 4, 6, 7, 8, (9), 10		Location indicated above (in green)
Mandible	W2 Postero-lateral	(2b), 3, 3a, 4, 5a, 6, 7a, 7b, 9b, 10b, (16)	NO ROHO	2, 2b, 3, 3a, 4, 5a, 5b, 6, 7a, 7b, 8a, 9b, 10a, 10b, 11, 16		
Mandible	F2 Postero-lateral	(1), 3, 6, 7, 8, 9, 10	(1), 3, 6, 7, 8, 10	3, 4, 6, 7, (9), 10		Location indicated above (in green)
Mandible	W3 Antero-medial	2b, (3), 3a, 4, 5a, 6, 7a, 7b, 9b, 10b	3, 4, 5a, 6, 7b, 8a, 9b, 10a, 11	NO ROHO		

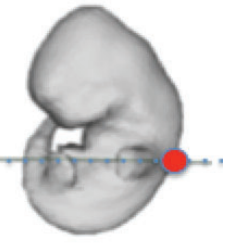
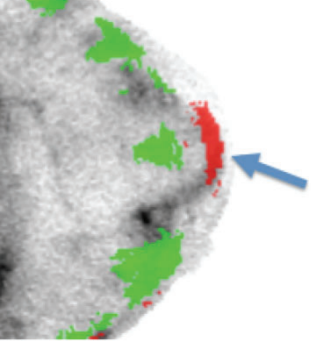
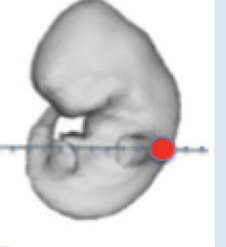
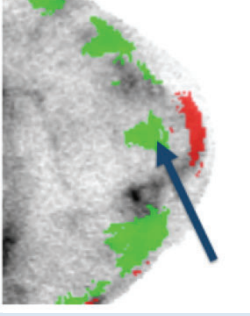
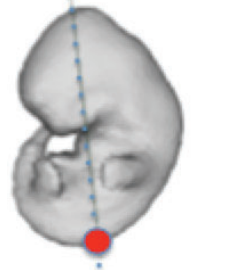
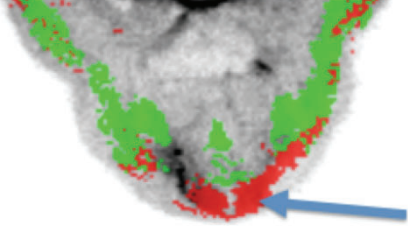
Mandible	F3 Antero-medial	3, 4, 6, 7, 8, 9, 10	1, 3, 6, 10	NO ROHO		Location indicated above (in green)
Arch 2	W4	(2b), 3, 3a, 4, 5a, (5b), 7a, 7b, 9b, 10b, (16)	NO ROHO	NO ROHO		
Arch 2	F4	(1), 3, 6, 7, 8, 9, 10	3, 4, 6, 7, 8, 10	1, 3, 4, (5), 6, 7, (8), (9), 10		Location indicated above (in green)
Neck	W5	No ROHO	2, 3, (4), 5a, 6, 7a, 9b, 10a, 11	2, 2b, 3, 3a, 4, 5a, 5b, 6, 7a, 7b, 8a, 9a, 9b, 10a, 10b, 11, 16		
Neck	F5	(1), 3, 4, (6), 7, 8, 9,	1, 3, (5), 6, 7, 8, (9), (10)	1, 3, 4, 5, 6, 7, 8, 9, 10		Location indicated above (in green)
Fore Limb	W6 Early distal E9.5 only	(2b), 3, 3a, 4, 5a, (5b), 6, 7a, 7b, (8b), 9b, 10a, 10b, 11, (16)				
Fore Limb	F6 Early distal E9.5 only	1, 3, 6, 7, 8, (9), 10				Location indicated above (in green)

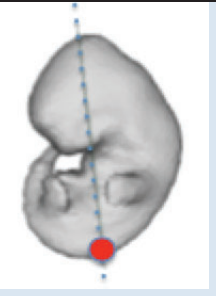
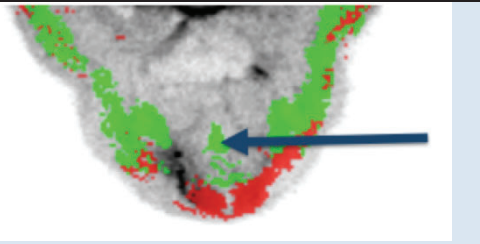
Fore Limb	W7 Distal	N/A	5a, 6, 7a, 10a, 10b, 11	NO ROHO		
Forelimb	F7 Distal	N/A	continuous with ROHO F10 (5), 6, 7, 8, 9, 10	NO ROHO		Location indicated above (in green)
Forelimb	W8 Proximo-ventral	No ROHO	2, 3, 4, 6, 7b, 8a, 9a, 9b, 10a, 10b, 11	2, 3, 3a, 4, 5a, 5b, 6, 7a, 7b, 8a, 9a, 9b, 10b, 11, (16)		
Forelimb	F8 Proximo-ventral	NO ROHO	1, 3, 6, 7, 10	1, 3, 5, 6, 7, 8, 10		Location indicated above (in green)
Forelimb	W9 Proximo-dorsal	NO ROHO	3, 4, 6, 10a, 10b, 11, 16	NO ROHO		
Forelimb	F9 Proximo-dorsal	NO ROHO	1, 3, 6, 7, 8, 10	1, (3), 4, (5), 6, 7, 8, 10		Location indicated above (in green)

Forelimb	W10 Dorsal surface	NO ROHO	NO ROHO	2, 2b, 3a, 4, 5a, 5b, 6, 7a, (7b), 8a, (9b), 10a, 10b, 11		
Forelimb	F10 Dorsal surface	NO ROHO	3, 6, 7, 8, (9), 10	1, (3), 4, 5, 6, 7, 8, 9, 10		Location indicated above (in green)
Flank	F11 Flank dorsal to fore limb	NO ROHO	1, 3, 6, 7, 8, 10	1, (3), (5), 6, 7, 8, (9), 10		
Flank	W12 Mid Flank	2, (2b), 3, (3a), 4, 5a, 6, 7a, 7b, 9b, (10a), 10b, 11 Small but distinct ROHO	NO ROHO	2, 2b, (3), 3a, 4, 5a, 5b, 6, 7a, (7b), 8a, (8b), 9a, 9b, (10a), 10b, 11, 16		
Flank	F12 Mid Flank	NO ROHO	3, 6, 7, 8, 10	1, 3, (4), 5, 6, 7, 8, 9, 10		Location indicated above (in green)

Ventral tail	W13	2b, 3, 3a, 4, 5a, 5b, (6), 7a, 7b, 11, 16	NO ROHO	2, (2b), 3, 3a, 4, 5a, 5b, 6, 7a, 7b, 9a, 9b, (10b), 16		
Ventral tail	F13	NO ROHO	NO ROHO	3, 6, 7, 9, 10		Location indicated above (in green)
Heart	W14 Right atrium	NO ROHO	NO ROHO	1, 2 2b, 3, 4, 5a, 5b, 6, 7a, 7b, 9a, 9b, 10a, 10b, 11, 16.		
Heart	W15 Left atrium	NO ROHO	NO ROHO	2, 3, 4, 5a, 5b, 6, 7a, 7b, 8a, 9a, 10a, 10b, 11, 16		

Cortical hem	W16	(1), 3a, 4, 5b, 7a, 7b, 8b, 9b, 10a 10b, (16)	NO ROHO	3,3a, 4,5a,5b,7a,7b,8a,8b,9a, 9b, 11,16		
Cortical hem	F16	NO ROHO	NO ROHO	3, 5, 6, 8, 9, 10		Location indicated above (in green)
Isthmus	W17	1, 5a, 5b, 7a, 7b, 10b	1, 3, (3a), 4, 5a, 5b, 7b	1, 2b, 3, 4, 5a, 5b, 7a, 7b, 8a, 8b, 9a, 9b, (10b), 11, 16		
Isthmus	F17	NO ROHO	3, (5), 6, 7, 9, 10,	1, 3, 5, 6, 7, 8, 9, (10)		Location indicated above (in green)
Midbrian	W18	1, 2b, 3, 3a, 4, (5a), 5b, 6, 7a, 7b, 10a, 10b	1, (2), 2b, 3, 3a, 4, 5a, 5b, 6, 7a, 7b, 8a, 8b, 9a, 9b, 10a, 10b, 11, 16,	1, 2b, 3, 3a, 4, 5a, 5b 6, 7a, 9a, 10a, 10b (11), 16		
Midbrian	F18	3, 6, 7, 8, 9, 10	1, 3, 4, 5, 6, 7, 8, 9, 10	1, 3, 4, 5, 6, 7, 8, 9, 10		Location indicated above (in green)

Dorsal anterior NT	W19	1, 3, 3a, 4, 7a, 7b, 10b, 16	1, 3, 4, (8a), 10a	1, 2b, 3, 3a, 4, 7a, 7b, 8a, 10a, 16,		
Dorsal anterior NT	F19	3, 6, 7, 8, (9), 10	3, (5), 6, 8, 10	NO ROHO		Location indicated above (in green)
Mid-d-v anterior NT	F20	NO ROHO	NO ROHO	3, 6, 7, 8, 10		
Dorsal trunk NT	W21	v. small ROHO 1, (3), 3a, 4, 7a, 7b, 9b, (10a)	1, 3, 3a, 4, 10a, 11	1, 2b, 3, 3a, 4, (5b), 7a, 7b, 10b		
Dorsal trunk NT	F21	3, (6), 7, 8, (9), 10	3, (5), 6, 7, 8, 10	NO ROHO		Location indicated above (in green)

Mid-ventral alar plate trunk NT	F22	NO ROHO	NO ROHO	3, 6, 7, 8, 9, 10		
---------------------------------------	------------	---------	---------	-------------------	---	---

In the Table above, the Wnt and Fzd ROHOs are numbered W1, W2, etc., F1, F2, etc. respectively. The location of each ROHO is illustrated at the latest stage the ROHO is present. **Bold** gene numbers indicate genes expressed in the ROHO at all stages when this ROHO is present. Gene numbers in parenthesis indicate that the expression domain or intersection with the ROHO is small, comprising only a few voxels. Note the number of genes listed can exceed the maximum occupancy for that ROHO because some genes intersect only part of the ROHO.

Table S4. Integrated Wnt expression patterns: Jaccard similarity indices for all gene expression domains for each stage. The full data is available as a Microsoft Excel file SuppTable3_AllData.xlsx.

Supplementary table 4a: E9.5 (Teiler 15), embryo ID EMA36

NAME	Wnt1	Wnt2	Wnt3	Wnt3a	Wnt4	Wnt5a	Wnt5b	Wnt6	Wnt7a	Wnt7b	Wnt8	Wnt9	Wnt10	Wnt10b	Wnt11	Wnt16	Fzd1	Fzd3	Fzd4	Fzd6	Fzd7	Fzd8	Fzd9	Fzd10	Tcf/Lef-GFP
Wnt1	1	0.000292	0.02141	0.12098	0.040274	0.039666	0.027792	0.02368	0.034837	0.022088	0.020363	0.000736	0.001333	0.000277	0.00001	0.000008	0.001524	0.002334	0.001251	0.02188	0.020228	0.023533	0.002981	0.007792	0.051334
Wnt2	0.000292	1	0.007707	0.005848	0.049788	0.030308	0.020243	0.022241	0.013397	0.001087	0.004344	0.002127	0.025201	0.010701	0.005608	0.001243	0.00231	0.019788	0.006133	0.023599	0.012412	0.013652	0.008432	0.009737	0.020977
Wnt3	0.021411	0.007707	1	0.027838	0.021391	0.026178	0.019986	0.044288	0.021496	0.001561	0.019761	0.001575	0.004366	0.009812	0.008438	0.004542	0.002398	0.001271	0.008848	0.0044	0.011036	0.005885	0.002021	0.010706	0.012569
Wnt3a	0.12098	0.005848	0.027838	1	0.143961	0.085149	0.028225	0.026451	0.079068	0.013204	0.017536	0.001661	0.011286	0.024461	0.013575	0.004702	0.008186	0.004102	0.004177	0.023704	0.012055	0.004126	0.011091	0.012077	0.071646
Wnt4	0.040274	0.049788	0.026178	0.085149	1	0.076379	0.024236	0.009004	0.077131	0.016025	0.011215	0.007103	0.00945	0.081133	0.015264	0.007849	0.00870	0.008204	0.019594	0.001614	0.089144	0.009516	0.070619	0.014491	0.012023
Wnt5a	0.039666	0.027792	0.019986	0.028225	0.076379	1	0.060112	0.048435	0.152887	0.014616	0.009079	0.016876	0.00031	0.011311	0.02551	0.002618	0.010385	0.150494	0.009375	0.008774	0.015796	0.011907	0.013529	0.025903	0.078303
Wnt5b	0.02368	0.020243	0.026451	0.028225	0.024236	0.060112	1	0.020623	0.029848	0.045317	0.008145	0.003157	0.012009	0.009587	0.005954	0.002023	0.001179	0.026246	0.005115	0.027264	0.005441	0.034882	0.025042	0.014646	0.044515
Wnt6	0.027792	0.021496	0.001561	0.019761	0.004366	0.009812	0.008438	1	0.074704	0.007785	0.003064	0.003888	0.005964	0.015867	0.005226	0.001574	0.018077	0.040205	0.012364	0.025219	0.074447	0.00746	0.076423	0.083748	0.081731
Wnt7a	0.022088	0.001087	0.000736	0.001333	0.000736	0.000277	0.000008	0.000001	0.000001	1	0.016501	0.018873	0.008828	0.017208	0.022398	0.001609	0.014543	0.040044	0.006105	0.011529	0.066056	0.118586	0.248579	0.08712	0.101513
Wnt7b	0.000736	0.001087	0.000736	0.001333	0.000736	0.000277	0.000008	0.000001	0.000001	0.016501	1	0.001582	0.026009	0.004561	0.00215	0.001104	0.000761	0.0115	0.001512	0.00617	0.00137	0.01243	0.003157	0.000941	0.014792
Wnt8	0.001333	0.001087	0.000736	0.001333	0.000736	0.000277	0.000008	0.000001	0.000001	0.018873	0.001582	1	0.000699	0.006999	0.001919	0.001356	0.001459	0.001137	0.010446	0.003205	0.01589	0.077787	0.054251	0.023553	0.030032
Wnt9	0.000736	0.001087	0.000736	0.001333	0.000736	0.000277	0.000008	0.000001	0.000001	0.003888	0.003888	0.000699	1	0.000699	0.001919	0.001356	0.001459	0.001137	0.010446	0.003205	0.01589	0.077787	0.054251	0.023553	0.030032
Wnt10	0.000277	0.000008	0.000001	0.000008	0.000001	0.000001	0.000001	0.000001	0.000001	0.008828	0.008828	0.000699	0.000699	1	0.000699	0.001919	0.001356	0.001459	0.001137	0.010446	0.003205	0.01589	0.077787	0.054251	0.023553
Wnt10b	0.000001	0.000008	0.000001	0.000008	0.000001	0.000001	0.000001	0.000001	0.000001	0.000699	0.000699	0.000699	0.000699	0.000699	1	0.000699	0.001919	0.001356	0.001459	0.001137	0.010446	0.003205	0.01589	0.077787	0.054251
Wnt11	0.000008	0.000001	0.000001	0.000008	0.000001	0.000001	0.000001	0.000001	0.000001	0.000699	0.000699	0.000699	0.000699	0.000699	0.000699	1	0.000699	0.001919	0.001356	0.001459	0.001137	0.010446	0.003205	0.01589	0.077787
Fzd1	0.001524	0.002334	0.001251	0.02188	0.020228	0.023533	0.002981	0.007792	0.051334	0.000008	0.001524	0.002334	0.001251	0.02188	0.020228	0.023533	1	0.00698	0.001826	0.009171	0.012073	0.01252	0.003149	0.021219	0.031448
Fzd3	0.002334	0.001251	0.02188	0.020228	0.023533	0.002981	0.007792	0.051334	0.000008	0.001524	0.002334	0.001251	0.02188	0.020228	0.023533	0.00698	1	0.009325	0.003637	0.024121	0.01653	0.004023	0.020023	0.004695	
Fzd4	0.001251	0.02188	0.020228	0.023533	0.002981	0.007792	0.051334	0.000008	0.001524	0.002334	0.001251	0.02188	0.020228	0.023533	0.00698	0.009325	0.003637	1	0.007093	0.007368	0.043877	0.028851	0.044701	0.009737	
Fzd6	0.023533	0.002981	0.007792	0.051334	0.000008	0.001524	0.002334	0.001251	0.02188	0.020228	0.023533	0.00698	0.009325	0.003637	0.007093	0.007368	0.043877	0.028851	1	0.007307	0.003129	0.0093129	0.0093129	0.0093129	
Fzd7	0.002981	0.007792	0.051334	0.000008	0.001524	0.002334	0.001251	0.02188	0.020228	0.023533	0.00698	0.009325	0.003637	0.007093	0.007368	0.043877	0.028851	0.007307	0.003129	1	0.0093129	0.0093129	0.0093129	0.0093129	
Fzd8	0.007792	0.051334	0.000008	0.001524	0.002334	0.001251	0.02188	0.020228	0.023533	0.00698	0.009325	0.003637	0.007093	0.007368	0.043877	0.028851	0.0093129	0.0093129	0.0093129	0.0093129	1	0.0093129	0.0093129	0.0093129	
Fzd9	0.051334	0.000008	0.001524	0.002334	0.001251	0.02188	0.020228	0.023533	0.00698	0.009325	0.003637	0.007093	0.007368	0.043877	0.028851	0.0093129	0.0093129	0.0093129	0.0093129	0.0093129	0.0093129	1	0.0093129		
Fzd10	0.007792	0.051334	0.000008	0.001524	0.002334	0.001251	0.02188	0.020228	0.023533	0.00698	0.009325	0.003637	0.007093	0.007368	0.043877	0.028851	0.0093129	0.0093129	0.0093129	0.0093129	0.0093129	0.0093129	1		
Tcf/Lef-GFP	0.001524	0.002334	0.001251	0.02188	0.020228	0.023533	0.002981	0.007792	0.051334	0.000008	0.001524	0.002334	0.001251	0.02188	0.020228	0.023533	0.00698	0.001826	0.009171	0.012073	0.01252	0.003149	0.021219	0.031448	

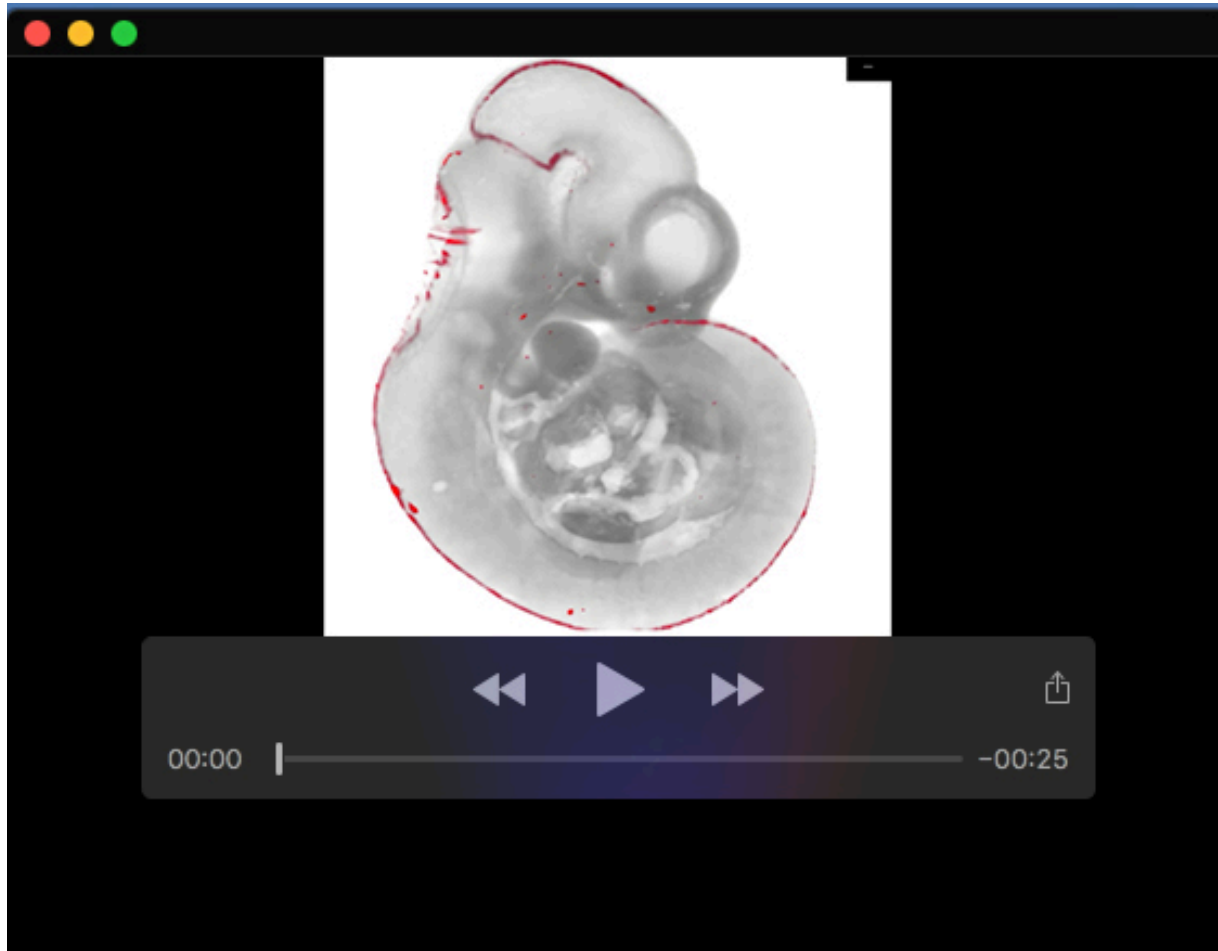
Supplementary table 4b: E10.5 (Teiler 18), embryo ID EMA31

NAME	Wnt1	Wnt2	Wnt3	Wnt3a	Wnt4	Wnt5a	Wnt5b	Wnt6	Wnt7a	Wnt7b	Wnt8	Wnt9	Wnt10	Wnt10b	Wnt11	Wnt16	Fzd1	Fzd3	Fzd4	Fzd6	Fzd7	Fzd8	Fzd9	Fzd10	Lef1	Tcf	Tcf1	Tcf2	Tcf3	Tcf4	Tcf5	Tcf6	Tcf7	Tcf8	Tcf9	Tcf10	Tcf11	Tcf12	Tcf13	Tcf14	Tcf15	Tcf16	Tcf17	Tcf18	Tcf19	Tcf20	Tcf21	Tcf22	Tcf23	Tcf24	Tcf25	Tcf26	Tcf27	Tcf28	Tcf29	Tcf30	Tcf31	Tcf32	Tcf33	Tcf34	Tcf35	Tcf36	Tcf37	Tcf38	Tcf39	Tcf40	Tcf41	Tcf42	Tcf43	Tcf44	Tcf45	Tcf46	Tcf47	Tcf48	Tcf49	Tcf50	Tcf51	Tcf52	Tcf53	Tcf54	Tcf55	Tcf56	Tcf57	Tcf58	Tcf59	Tcf60	Tcf61	Tcf62	Tcf63	Tcf64	Tcf65	Tcf66	Tcf67	Tcf68	Tcf69	Tcf70	Tcf71	Tcf72	Tcf73	Tcf74	Tcf75	Tcf76	Tcf77	Tcf78	Tcf79	Tcf80	Tcf81	Tcf82	Tcf83	Tcf84	Tcf85	Tcf86	Tcf87	Tcf88	Tcf89	Tcf90	Tcf91	Tcf92	Tcf93	Tcf94	Tcf95	Tcf96	Tcf97	Tcf98	Tcf99	Tcf100	Tcf101	Tcf102	Tcf103	Tcf104	Tcf105	Tcf106	Tcf107	Tcf108	Tcf109	Tcf110	Tcf111	Tcf112	Tcf113	Tcf114	Tcf115	Tcf116	Tcf117	Tcf118	Tcf119	Tcf120	Tcf121	Tcf122	Tcf123	Tcf124	Tcf125	Tcf126	Tcf127	Tcf128	Tcf129	Tcf130	Tcf131	Tcf132	Tcf133	Tcf134	Tcf135	Tcf136	Tcf137	Tcf138	Tcf139	Tcf140	Tcf141	Tcf142	Tcf143	Tcf144	Tcf145	Tcf146	Tcf147	Tcf148	Tcf149	Tcf150	Tcf151	Tcf152	Tcf153	Tcf154	Tcf155	Tcf156	Tcf157	Tcf158	Tcf159	Tcf160	Tcf161	Tcf162	Tcf163	Tcf164	Tcf165	Tcf166	Tcf167	Tcf168	Tcf169	Tcf170	Tcf171	Tcf172	Tcf173	Tcf174	Tcf175	Tcf176	Tcf177	Tcf178	Tcf179	Tcf180	Tcf181	Tcf182	Tcf183	Tcf184	Tcf185	Tcf186	Tcf187	Tcf188	Tcf189	Tcf190	Tcf191	Tcf192	Tcf193	Tcf194	Tcf195	Tcf196	Tcf197	Tcf198	Tcf199	Tcf200	Tcf201	Tcf202	Tcf203	Tcf204	Tcf205	Tcf206	Tcf207	Tcf208	Tcf209	Tcf210	Tcf211	Tcf212	Tcf213	Tcf214	Tcf215	Tcf216	Tcf217	Tcf218	Tcf219	Tcf220	Tcf221	Tcf222	Tcf223	Tcf224	Tcf225	Tcf226	Tcf227	Tcf228	Tcf229	Tcf230	Tcf231	Tcf232	Tcf233	Tcf234	Tcf235	Tcf236	Tcf237	Tcf238	Tcf239	Tcf240	Tcf241	Tcf242	Tcf243	Tcf244	Tcf245	Tcf246	Tcf247	Tcf248	Tcf249	Tcf250	Tcf251	Tcf252	Tcf253	Tcf254	Tcf255	Tcf256	Tcf257	Tcf258	Tcf259	Tcf260	Tcf261	Tcf262	Tcf263	Tcf264	Tcf265	Tcf266	Tcf267	Tcf268	Tcf269	Tcf270	Tcf271	Tcf272	Tcf273	Tcf274	Tcf275	Tcf276	Tcf277	Tcf278	Tcf279	Tcf280	Tcf281	Tcf282	Tcf283	Tcf284	Tcf285	Tcf286	Tcf287	Tcf288	Tcf289	Tcf290	Tcf291	Tcf292	Tcf293	Tcf294	Tcf295	Tcf296	Tcf297	Tcf298	Tcf299	Tcf300	Tcf301	Tcf302	Tcf303	Tcf304	Tcf305	Tcf306	Tcf307	Tcf308	Tcf309	Tcf310	Tcf311	Tcf312	Tcf313	Tcf314	Tcf315	Tcf316	Tcf317	Tcf318	Tcf319
------	------	------	------	-------	------	-------	-------	------	-------	-------	------	------	-------	--------	-------	-------	------	------	------	------	------	------	------	-------	------	-----	------	------	------	------	------	------	------	------	------	-------	-------	-------	-------	-------	-------	-------	-------	-------	-------	-------	-------	-------	-------	-------	-------	-------	-------	-------	-------	-------	-------	-------	-------	-------	-------	-------	-------	-------	-------	-------	-------	-------	-------	-------	-------	-------	-------	-------	-------	-------	-------	-------	-------	-------	-------	-------	-------	-------	-------	-------	-------	-------	-------	-------	-------	-------	-------	-------	-------	-------	-------	-------	-------	-------	-------	-------	-------	-------	-------	-------	-------	-------	-------	-------	-------	-------	-------	-------	-------	-------	-------	-------	-------	-------	-------	-------	-------	-------	-------	--------	--------	--------	--------	--------	--------	--------	--------	--------	--------	--------	--------	--------	--------	--------	--------	--------	--------	--------	--------	--------	--------	--------	--------	--------	--------	--------	--------	--------	--------	--------	--------	--------	--------	--------	--------	--------	--------	--------	--------	--------	--------	--------	--------	--------	--------	--------	--------	--------	--------	--------	--------	--------	--------	--------	--------	--------	--------	--------	--------	--------	--------	--------	--------	--------	--------	--------	--------	--------	--------	--------	--------	--------	--------	--------	--------	--------	--------	--------	--------	--------	--------	--------	--------	--------	--------	--------	--------	--------	--------	--------	--------	--------	--------	--------	--------	--------	--------	--------	--------	--------	--------	--------	--------	--------	--------	--------	--------	--------	--------	--------	--------	--------	--------	--------	--------	--------	--------	--------	--------	--------	--------	--------	--------	--------	--------	--------	--------	--------	--------	--------	--------	--------	--------	--------	--------	--------	--------	--------	--------	--------	--------	--------	--------	--------	--------	--------	--------	--------	--------	--------	--------	--------	--------	--------	--------	--------	--------	--------	--------	--------	--------	--------	--------	--------	--------	--------	--------	--------	--------	--------	--------	--------	--------	--------	--------	--------	--------	--------	--------	--------	--------	--------	--------	--------	--------	--------	--------	--------	--------	--------	--------	--------	--------	--------	--------	--------	--------	--------	--------	--------	--------	--------	--------	--------	--------	--------	--------	--------	--------	--------	--------	--------	--------	--------	--------	--------	--------	--------	--------

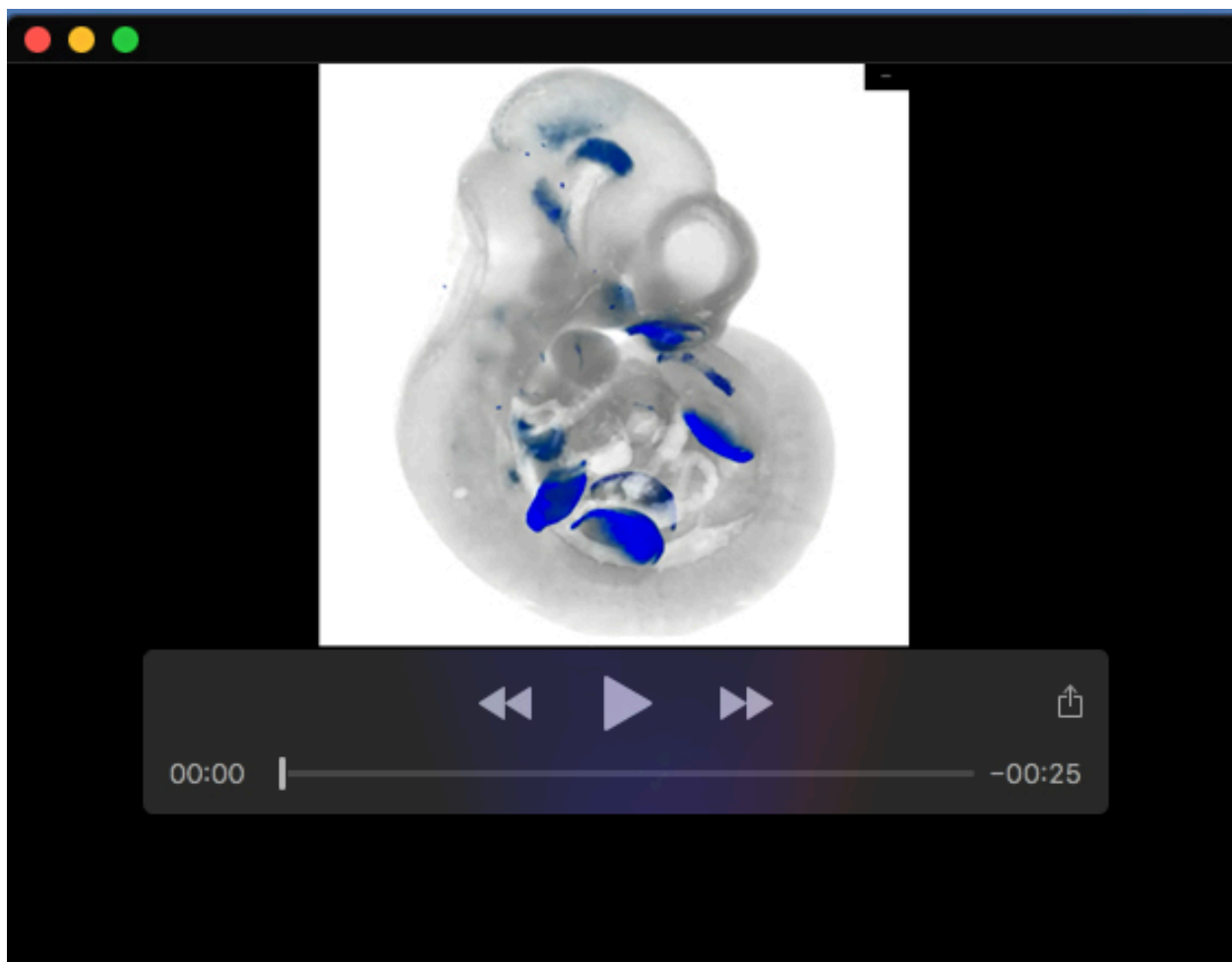
Table S5. details of gene expression probes and EMAGE entry IDs

*Note no specific expression detected for Fzd2 and Sfrp5 at these stages

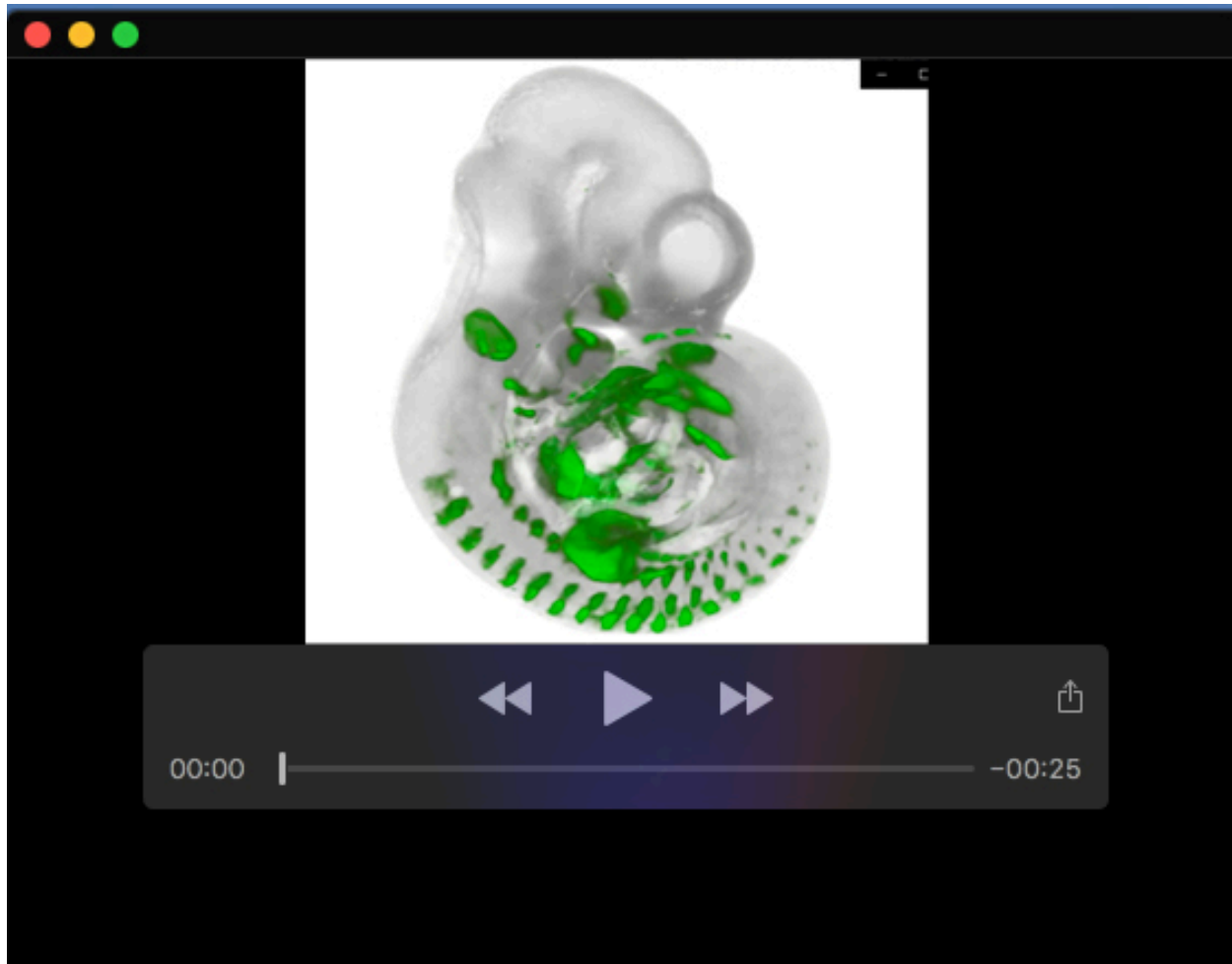
Gene	Extent of Probe on Genbank Sequence	Source	EMAGE IDs
Wnt1	Nucleotide 138 to 2345 on genbank sequence BC005449.1	A. McMahon	EMAGE:6131 EMAGE:6132 EMAGE:3949
Wnt2	Nucleotide 19 to 1493 on genbank sequence BC026373	A. McMahon	EMAGE:6133 EMAGE:6134 EMAGE:3950
Wnt2b	Nucleotide 882 to 1103 on genbank sequence AF070988	L. Zakin	EMAGE:6135 EMAGE:6136 EMAGE:3951
Wnt3	Nucleotide 1610 to 2973 on genbank sequence NM_009521.1	P. Salinas	EMAGE:6137 EMAGE:6138 EMAGE:3952
Wnt3a	Nucleotide 2310 to 2676 on genbank sequence NM_009522.1	RT-PCR generated	EMAGE:6139 EMAGE:6141 EMAGE:3953
Wnt4	Nucleotide 853 to 1315 on genbank sequence AK012727	A. McMahon	EMAGE:6140 EMAGE:6142 EMAGE:3954
Wnt5a	Nucleotide 193 to 2324 on genbank sequence BC018425	A. McMahon	EMAGE:6143 EMAGE:6144 EMAGE:3955
Wnt5b	Nucleotide 111 to 1429 on genbank sequence BC010775	A. McMahon	EMAGE:6145 EMAGE:6146 EMAGE:3956
Wnt6	Nucleotide 27 to 2066 on genbank sequence NM_009526.3	A. McMahon	EMAGE:6147 EMAGE:6148 EMAGE:3957
Wnt7a	Nucleotide 24 to 3164 on genbank sequence BC049093	A. McMahon	EMAGE:6149 EMAGE:6150 EMAGE:3958
Wnt7b	Nucleotide 93 to 1581 on genbank sequence NM_009528.2	A. McMahon	EMAGE:6151 EMAGE:6152 EMAGE:3959
Wnt8a	Nucleotide 87 to 1746 on genbank sequence NM_009290.1	P. Chambon	EMAGE:6153 EMAGE:3960
Wnt8b	Nucleotide 942 to 1631 on genbank sequence NM_011720.2	J. Mason	EMAGE:6166 EMAGE:6154 EMAGE:3961
Wnt9a	Nucleotide 1698 to 2247 on genbank sequence NM_139298.2	RT-PCR generated	EMAGE:6155 EMAGE:6156 EMAGE:3962
Wnt9b	Nucleotide 2834 to 3436 on genbank sequence NM_011719.3	RT-PCR generated	EMAGE:6158 EMAGE:6157 EMAGE:3963
Wnt10a	Nucleotide 289 to 2469 on genbank sequence NM_009518.1	IMAGE clone	EMAGE:6159 EMAGE:6160 EMAGE:3964
Wnt10b	Nucleotide 27 to 473 on genbank sequence U61970	A. McMahon	EMAGE:6167 EMAGE:6161 EMAGE:3965
Wnt11	Nucleotide 169 to 1789 on genbank sequence NM_009519.1 + 419bp of 3' UTR	A. McMahon	EMAGE:6162 EMAGE:6163 EMAGE:3966
Wnt16	Nucleotide 538 to 1532 on genbank sequence NM_053116	PCR cloned	EMAGE:6164 EMAGE:6165 EMAGE:3967
Fzd1	Nucleotide 2774 to 3663 on genbank sequence NM_021457.2	PCR cloned	EMAGE:6129 EMAGE:6130 EMAGE:3939
Fzd2*	Nucleotide 3106 to 3441 on genbank sequence BC049774	IMAGE clone	Not detected
Fzd3	Nucleotide 127 to 1485 on genbank sequence BC050965	U. Borello/C. Cossu	EMAGE:6101 EMAGE:6115 EMAGE:3941
Fzd4	Nucleotide 1419 to 1862 on genbank sequence BC015256	U. Borello/C. Cossu	EMAGE:6116 EMAGE:6117 EMAGE:3942
Fzd5	Nucleotide 640 to 868 on genbank sequence AB052910	U. Borello/C. Cossu	EMAGE:6118 EMAGE:6119 EMAGE:3943
Fzd6	Nucleotide 1794 to 2642 on genbank sequence NM_008056.2	U. Borello/C. Cossu	EMAGE:6120 EMAGE:6121 EMAGE:3944
Fzd7	Nucleotide 191 to 1013 on genbank sequence BC049781	U. Borello/C. Cossu	EMAGE:6122 EMAGE:6123 EMAGE:3945
Fzd8	Nucleotide 968 to 1965 on genbank sequence NM_008058.1	U. Borello/C. Cossu	EMAGE:6124 EMAGE:6125 EMAGE:3946
Fzd9	Nucleotide 678 to 1178 on genbank sequence AF033585	U. Borello/C. Cossu	EMAGE:6126 EMAGE:3947
Fzd10	Nucleotide 1892 to 2988 on genbank sequence NM_175284.3	IMAGE library	EMAGE:6127 EMAGE:6128 EMAGE:3948
Lef1	Nucleotide 371 on NM_010703.3	J. Meeldijk	EMAGE:5753 (TS16) EMAGE:5757 EMAGE:5758
Tcf7	Nucleotide 18 to 1572 on NM_009331.3	R.Grosschedl	EMAGE:5765 EMAGE:5759 EMAGE:5760
Tcf7I1	Nucleotide 86 to 1582 on NM_009332.2	Cloned: library screen	EMAGE:5766 EMAGE:5761 EMAGE:5762
Tcf7I2	Nucleotide 946 to 1361 on NM_009333.3	J.Rubenstein	EMAGE:5754 (TS16) EMAGE:5763 EMAGE:5764
β-catenin	Nucleotide 2194 to 2621 on NM_007614.2	U.Borello/ G. Cossu	EMAGE 5752 EMAGE 5755 EMAGE 5756
Sfrp1	Nucleotide 12 to 784 on NM_013834	A Rattner	Not on EMAGE
Sfrp2	Nucleotide 82 to 852 on U88569	A Rattner	"
Sfrp3	Nucleotide 2059-2522 on NM_011356.4	PCR cloned	"
Sfrp4	Nucleotide 9 to 1756 on NM_016687.3	A Rattner	"
Sfrp5*	Nucleotide 1 to 1081 on NM_018780.3	PCR cloned	Not detected
Wif1	Nucleotide 876 to 2237 on NM_011915.2	IMAGE library	Not on EMAGE
Wise	Nucleotide 81 to 1038 on NM_025312.3	IMAGE library	"
Ror2	Nucleotide 1 to 3968 on NM_013846.3	IMAGE library	"



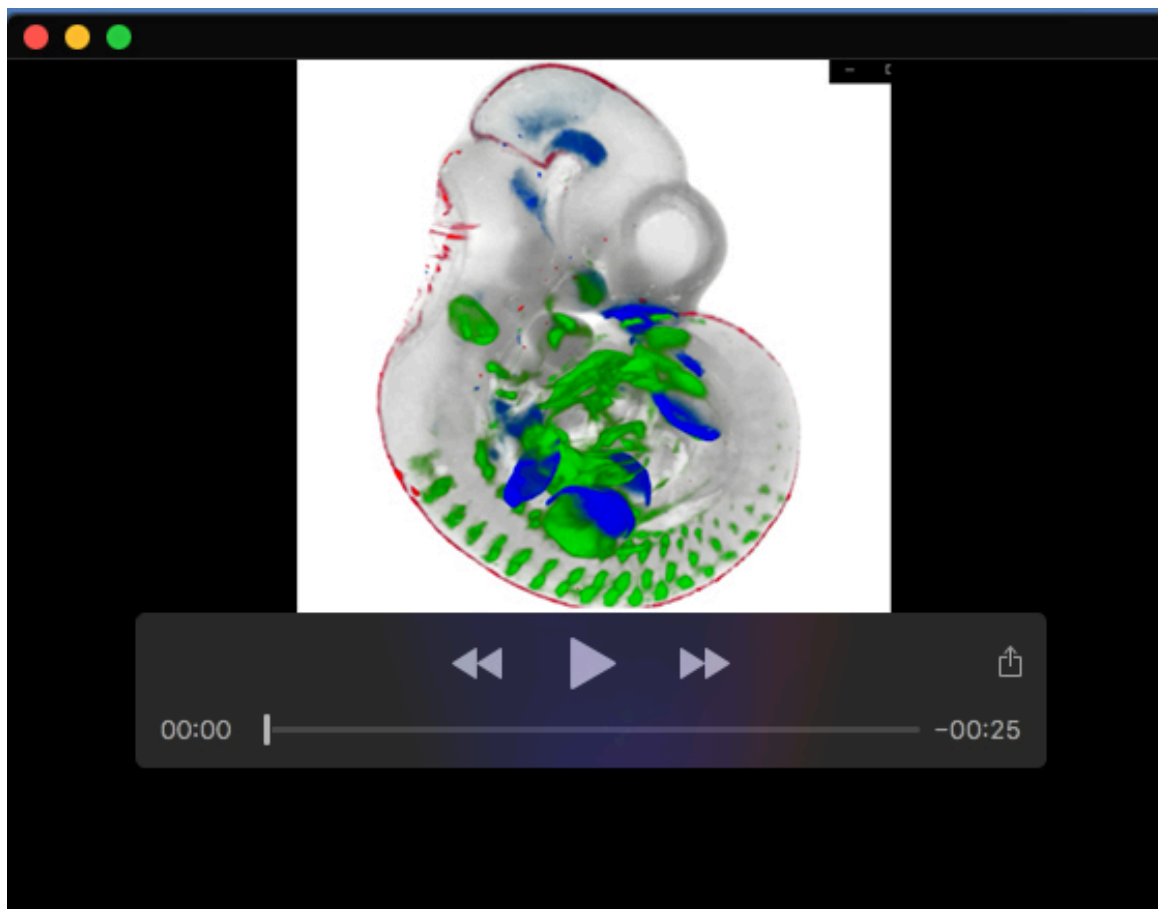
Movie 1. 3D movie of Wnt1 expression pattern at E10.5 mapped onto reference embryo



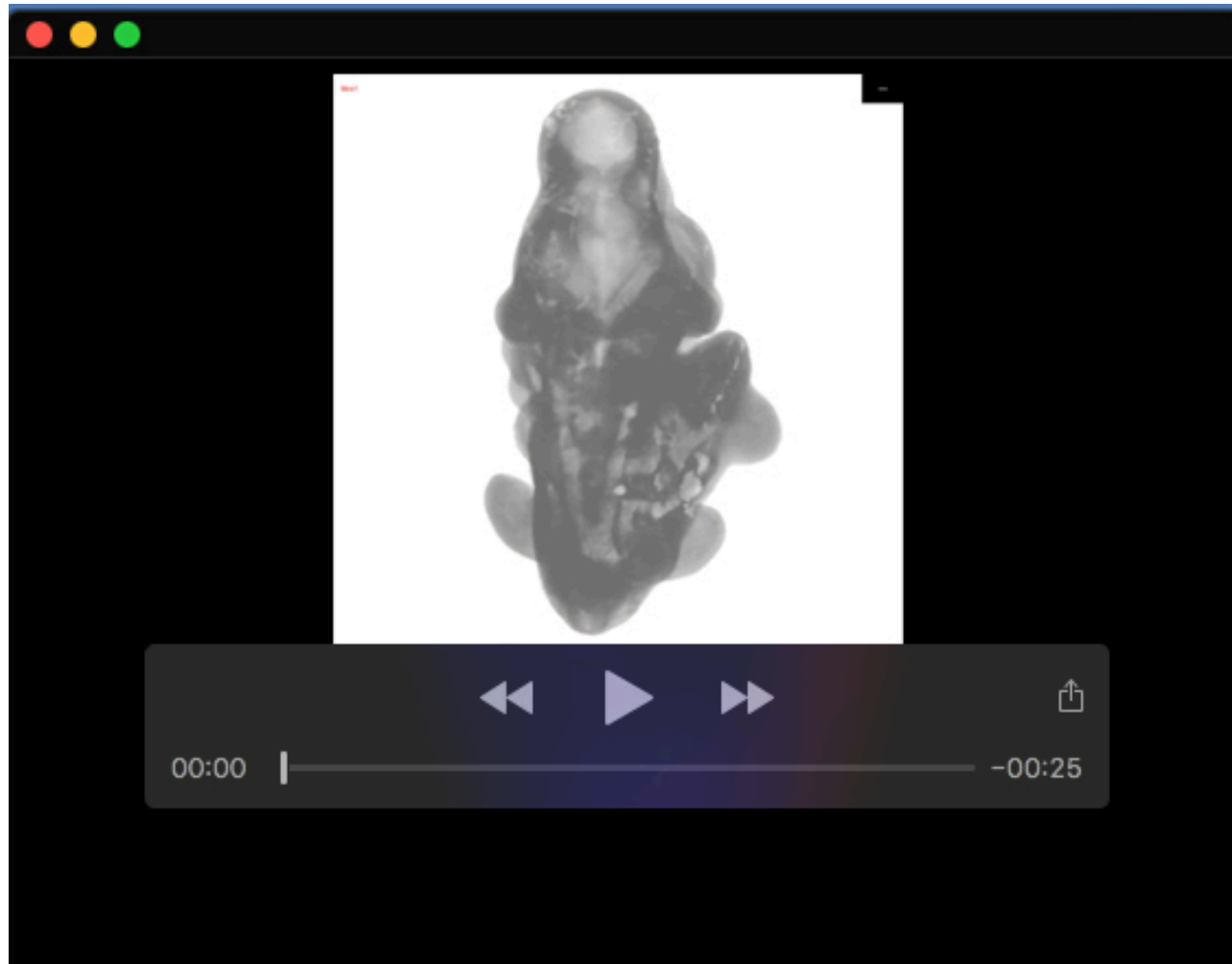
Movie 2. 3D movie of Wnt5a expression pattern at E10.5 mapped onto reference embryo



Movie 3. 3D movie of Wnt11 expression pattern at E10.5 mapped onto reference embryo



Movie 4. 3D movie of integrated Wnt1 (red), Wnt5a (blue) and Wnt11 (green) expression patterns at E10.5 mapped onto reference embryo



Movie 5. 3D movie of integrated expression patterns of all 19 Wnt genes (colour codes indicated on movie) at E10.5 mapped onto reference embryo.